

# An Adaptive Sequential Experimentation Methodology for Expensive Response Surface Optimization – Case Study in Traumatic Brain Injury Modeling

Adel Alaeddini,<sup>a,\*†</sup> Kai Yang,<sup>b</sup> Haojie Mao,<sup>c</sup> Alper Murat<sup>d</sup>  
and Bruce Ankenman<sup>e</sup>

The preset response surface designs often lack the ability to adapt the design based on the characteristics of application and experimental space so as to reduce the number of experiments necessary. Hence, they are not cost effective for applications where the cost of experimentation is high or when the experimentation resources are limited. In this paper, we present an adaptive sequential methodology for  $n$ -dimensional response surface optimization ( $n$ -dimensional adaptive sequential response surface methodology (N-ASRSM)) for industrial experiments with high experimentation cost, which requires high design optimization performance. We also develop a novel risk adjustment strategy for effectively considering the effect of noise into the design. The N-ASRSM is a sequential adaptive experimentation approach, which uses the information from previous experiments to design the subsequent experiment by simultaneously reducing the region of interest and identifying factor combinations for new experiments. Its major advantage is the experimentation efficiency such that, for a given response target, it identifies the input factor combination in less number of experiments than the classical response surface methodology designs. We applied N-ASRSM to the problem of traumatic brain injury modeling and compared the result with the conventional central composite design. Also, through extensive simulated experiments with different quadratic and nonlinear cases, we show that the proposed N-ASRSM method outperforms the classical response surface methodology designs and compares favorably with other sequential response surface methodologies in the literature in terms of both design optimality and experimentation efficiency. Copyright © 2013 John Wiley & Sons, Ltd.

**Keywords:** adaptive sequential response surface optimization; simplex optimization; risk adjustment; fractional factorial design; central composite design (CCD)

## 1. Introduction

Response surface methodology (RSM) is an experimental method used to locate an improved set of conditions for a process or a design. RSM was introduced by Box and Wilson<sup>1</sup> and its essential elements have remained unchanged:

1. Perform a first-order design and fit linear model (often a fractional factorial design)
2. Follow the path of steepest ascent until an area of curvature is reached
3. Perform a second-order design (often a central composite design built from a new factorial design)
4. Fit a quadratic model to locate at least a local optimum where conditions are improved.

Figure 1(a) shows the RSM algorithm graphically in a two-dimensional example from Box *et al.*<sup>2</sup>. Here, RSM is used to find settings of time and temperature that improve the yield of a chemical process. Each number on the plot represents an experiment and the resulting observation of the process yield at that set of conditions. Initially, time is set near 74 min and temperature is set near 130° with a resulting

<sup>a</sup>Department of Mechanical Engineering, University of Texas at San Antonio, TX 78230, USA

<sup>b</sup>Department of Industrial and Systems Engineering, Wayne State University, MI 48202, USA

<sup>c</sup>Bioengineering Center, Wayne State University, MI 48202, USA

<sup>d</sup>Department of Industrial and Systems Engineering, Wayne State University, MI 48202, USA

<sup>e</sup>Department of Industrial Engineering & Management Sciences, Northwestern University, Evanston, IL 60208, USA

\*Correspondence to: Adel Alaeddini, Ph.D. Assistant Professor of Mechanical Engineering, Department of Mechanical Engineering, University of Texas at San Antonio, TX 78230, USA.

†E-mail: adel.alaeddini@utsa.edu

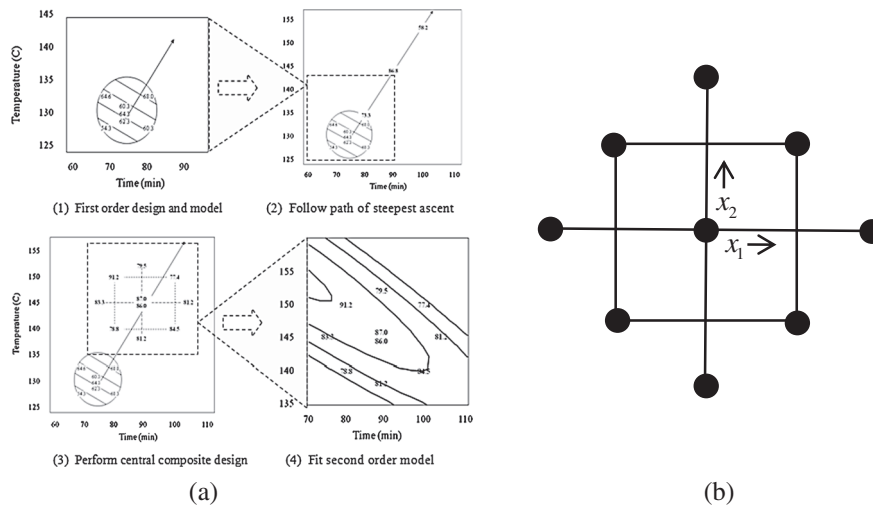


**Figure 1.** (a) The basic response surface methodology process illustrated for a two-dimensional chemical process example and (b) a central composite design in two dimensions

yield of around 60–65. At the end of the RSM algorithm, a yield near 90 is achieved by setting time to 80 min and temperature to 150°. Slight additional improvement might be made by following the second-order surface higher in temperature and lower in time.

In two dimensions, the full second-order model only has six terms,

$$y = \beta_0 + \beta_1x_1 + \beta_2x_2 + \beta_{12}x_1x_2 + \beta_{11}x_1^2 + \beta_{22}x_2^2 \quad (1)$$

and the central composite design (CCD) has only as nine design points. The central composite design is built by combining a factorial design (the four corner points), with four star points on the axes and a center point as shown in Figure 1(b). In the chemical example, the center point was replicated to estimate measurement variability. However, as dimensions increase, the number of terms in the quadratic model and the number of design points in the central composite design become infeasible (Table I).

There are many approaches for decreasing the experimental effort for the fitting of the quadratic model including reducing the size of the central composite design to support only second-order terms<sup>3</sup> or using the more efficient Box–Behnken design (BBD).<sup>4</sup> Other methods use an optimality criterion for building an experimental design that optimally supports the fitting of the quadratic model. To locate the optimum, most of these methods require that an experimental design be built that will support the estimation of all terms in the second-order model and thus must have at least that many design points. Typically the design is built in two steps, the first fits first-order model and the second fits the second-order model. However, most methods do not use a sequential design that places new design points adaptively in a way that may locate the optimum before the second-order model is estimable.

The purpose of this study is to provide a new, adaptive, and extremely data efficient method for accomplishing the last two steps of RSM. More specifically, the goal is to find an optimum in a local region of interest where a quadratic model is a reasonably good approximation. The method is intended to be highly efficient, locating the optimum with as few observations as possible – often before the second-order model is fully estimable. The algorithm is sequential, adaptive, and recursive with the following steps: (i) split up the feasible region into hyper-rectangular subregions; (ii) eliminate subregions that are unlikely to contain the optimum; and then (iii) iterate back to step one to subdivide the remaining feasible regions into smaller hyper-rectangular sub-subregions. Eventually, the remaining feasible subregion is small enough to declare it the optimum.

In what follows, we briefly review the literature on advancements in RSM with special emphasis on the adaptive experimentation methodologies in Section 2. Section 3 presents the proposed *n*-dimensional adaptive sequential response surface (N-ASRSM) methodology in detail. In Section 4, we present the results of applying the N-ASRSM method to the stylized and real world experiments and compare with those of the optimal designs, classical BBD and CCD, and some sequential design in the literature. Finally, Section 5 discusses results and presents future research directions.

**Table I.** The increase in the number of terms in the quadratic model and number of design points in central composite design as the dimensions increases

Number of dimensions	Terms in second-order model	Design points in central composite design
3	10	15
4	15	25
5	21	43
6	28	77
7	36	143
8	45	273

## 2. Response surface methodology literature

This section presents the relevant literature for the proposed adaptive experimental design methodology. We first review the classical response surface methodologies and then more advanced methods including optimal design, Bayesian design, and incomplete design strategies. Finally, we briefly describe other adaptive design methodologies such as steepest ascent, simplex-based methods, evolution operation methods, adaptive one-factor-at-a-time (AOFAT) methods, adaptive RSM, sequential RSM, and sequential and adaptive approximation methods from the engineering design domain.

Response surface methodology has been used as one of the most effective tools for process and product development since its introduction by Box and Wilson<sup>1</sup>. RSM consists of statistical and numerical/mathematical optimization techniques for examining the relationship between one or more response variables and a set of quantitative experimental variables or factors. Because the literature on RSM is vast, we herein refer the reader to a number of good review studies. Box<sup>5</sup> provides a retrospective on the origins of RSM with a general philosophy of sequential learning. Myers *et al.*<sup>6</sup> present a thorough discussion of RSM from 1966 to 1988. Myers<sup>7</sup> discusses the RSM state in late 1990s and gives some directions for future research. Myers *et al.*<sup>8</sup> presents a retrospective and literature survey on RSM.

Central composite design and BBD are the most popular class of designs used for fitting second-order model.<sup>4</sup> Generally, the CCD consists of a factorial or fractional factorials of resolution with runs, axial or star runs, and center points. There are usually two parameters in CCD that must be specified: the distance of the axial runs from the design center and the number of center points. It is common to set  $\alpha = (n_F)^{1/4}$  to make the design rotatable. Also three to five runs are recommended in the literature.<sup>9</sup> The number of runs in CCD increases exponentially with the number of design variables and hence, becomes inefficient for high dimensional design problems. One alternative to CCD is small composite designs that consist of a fraction of CCD points.<sup>10</sup> However, the small composite design has significant difficulty in estimating linear and interaction coefficients.<sup>11</sup> BBD is another design approach, which requires  $n \geq 3$ .<sup>4</sup> BBD is formed by combining  $2^n$  factorials with incomplete block designs. This design does not contain any points at the vertices of the region created by the upper and lower limits for each variable.

Optimal design methodologies select designs, which are *best* with respect to some criterion. This selection process includes: specifying the model; determining the region of interest, selecting the number of runs to make, specifying the optimality criterion, and choosing the design points from a set of candidate points spaced over the feasible design region. Kiefer<sup>12,13</sup> and Kiefer and Wolfowitz<sup>14</sup> greatly contribute to the development of the idea of optimal designs. *D*-optimal design is the most widely used criterion in optimal designs. A design is said to be *D*-optimal if  $|[X'X]^{-1}|$  is minimized. This is equivalent to minimizing the volume of the joint confidence region of the vector of regression coefficients. Andere-Rendon *et al.*<sup>15</sup> use *D*-optimal design for mixture experiments. There are also other types of optimal designs such as *A*-optimal design, which deals with only the variance of the regression coefficients, *G*-optimal design that minimizes the maximum scaled prediction variance over the design region, and *V*-optimal design that minimizes the average prediction variance over the set of *m* points of interest.

Box and Wilson<sup>1</sup> suggest a two-stage sequential CCD where the first stage is a two-level factorial or fractional factorial design, and the axial points constitute the second stage. The axial points are then used if the lack-of-fit test indicates curvature in the system. The method of steepest ascent<sup>1</sup> is another adaptive sequential experimentation approach in which the experimental points move sequentially along the gradient direction. Joshi *et al.*<sup>16</sup> applied a deflected conjugate gradient approach to improve the performance of RSM. Kleijnen *et al.*<sup>17,18</sup> combine mathematical statistics and mathematical programming techniques to overcome two problems of steepest ascent algorithm in RSM, that is, scale-dependent steepest ascent as well as intuitive selection of step size. Evolutionary operation, another adaptive experimental approach, iteratively builds a response surface around the optimum from the previous iteration by drifting factorial experiments with center points.<sup>19,20</sup> Both these approaches are primarily used for shifting the region of interest close to the optimum and replicate the same experimental design iteratively in different regions of the factor space. Spendley *et al.*<sup>21</sup> discuss the sequential application of simplex designs in optimization and evolutionary operation. They propose using a simplex pattern instead of a factorial pattern as in Box<sup>19</sup>. A simplex is an  $n + 1$  dimensional form in  $n$  dimensions, for example, a triangle in two dimensions and a tetrahedron in three dimensions. They present a simplex search method where a sequence of experimental designs in the form of a regular or irregular simplex is used.

One-factor-at-a-time (OFAT) can be considered as the earliest adaptive sequential experimentation approach proposed.<sup>22</sup> OFAT changes one variable at a time while keeping others constant at fixed values to find the best response. Once a factor is changed, its value is fixed in the remainder of the process. This process is repeated until all the variables are tried. However, OFAT experimentation is generally discouraged in the literature on the experimental design in comparison with factorial design and fractional factorial design. Box *et al.*<sup>2</sup> and Montgomery<sup>9</sup> talk about advantages of factorial experiment over OFAT experimentation. Czitrom<sup>23</sup> write in favor of factorial experiment over OFAT experiments in terms of finding the behavior of the system. Frey *et al.*<sup>24</sup> introduce AOFAT experimentation method. They compare AOFAT technique with orthogonal arrays through computer simulations and concluded that AOFAT technique tends to achieve greater gains than those of orthogonal arrays when experimental error is small or the interactions among control factors are large. Frey and Jugulum<sup>25</sup> investigate the mechanisms by which AOFAT technique led to improvement. The parameters that they investigated were conditional main effect, exploitation of an effect, synergistic interaction, antisnergistic interaction, and overwhelming effect. Frey and Wang<sup>26</sup> present the models of AOFAT and factor effects and illustrate with theorems that AOFAT method exploits main effects if interactions are small and exploits two-factor interactions when two-factor interactions are large.

Wang *et al.*<sup>27</sup> develop an adaptive RSM methodology, called adaptive response surface method (ARSM). ARSM is a sequential experimentation method, where at each iteration, ARSM discards portions of the design space that correspond to the response values worse than a given threshold value. Such elimination reduces the design space gradually to the neighborhood of the global

design optimum. ARSM performs a CCD experiment at each iteration, and thus the number of required design experiments increases exponentially with the number of design variables. Further ARSM does not inherit any of the previous runs and requires a completely new set of CCD points. Wang<sup>28</sup> proposes a modified ARSM where the CCD is substituted with Latin hypercube design. Sandler<sup>29</sup> proposes the successive RSM method, which uses a region of interest, a subspace of the design space, to determine an approximate optimum. A range is chosen for each variable to determine its initial size. Then a new region of interest is centrally built on each successive optimum. The improvement in response is attained by moving the center of the region of interest as well as reducing its size through panning and zooming operations, respectively. At each subregion, a D-optimal experimental design is used to best utilize the number of available runs together with over sampling to maximize the predictive capability. Moore *et al.*<sup>30</sup> suggest an algorithm, known as Q2, for optimizing the expected output of a multi-input noisy continuous function. Q2 is designed to need only a few experiments and avoids strong assumptions on the form of the function. Their algorithm uses instance-based determination of a convex region of interest for performing experiments. To define a neighborhood, they use a geometric procedure that captures the size and shape of the zone of possible optimum location/s. Their algorithm also tries to optimize weighted combinations of outputs and finds inputs to produce target outputs. Anderson *et al.*<sup>31</sup> develop a nonparametric approach called pairwise bisection for optimizing expensive noisy function with few function evaluations. Their algorithm uses nonparametric reasoning about simple geometric relationships to find minima efficiently. They use nonparametric statistics because for its independence from the traditional assumptions of continuousness and Gaussian noise. They also used pairwise bisection as an attempt to automate the process of robust and efficient experiment design. Alaeddini *et al.*<sup>32</sup> develop a methodology of adaptive sequential experiment for two-dimensional responses, which uses previous experiments information for determining the factor settings of new experiments, and shrinks the factor space to a smaller region toward the optimal point. Their proposed methodology combines an extension of golden section search method in nonlinear optimization and classical response surface optimization for reducing the number of required experiments for estimating the optimal point. Alaeddini *et al.*<sup>33</sup> propose an adaptive methodology, which integrates typical optimal design of experiments with a nonparametric strategy for efficient estimation of optimal point in high-dimensional response surfaces. They also show that their methodology performs acceptable on quadratic and nonlinear responses.

Another adaptive and sequential experimentation research stream emerges from the engineering design community. In the engineering design, computation-intensive design analyses are commonly expensive computer *experiments* and thus require experimental optimization for design optimization. The response surface models based on computer experiments are called *surrogates* and commonly used in multidisciplinary design optimization. Sobieszczanski-Sobieski<sup>34</sup> proposes concurrent subspace optimizations (CSSO) where the multidisciplinary systems are linearly decoupled for concurrent optimization. Renaud and Gabriele<sup>35</sup> modify this algorithm to build response surface approximations of the objective function and the constraints. Rodríguez *et al.*<sup>36</sup> introduce a general framework for surrogate optimization with a trust region approach. Jones *et al.*<sup>37</sup> propose an efficient global optimization (EGO) of expensive black-box functions. Alexandrov *et al.*<sup>38</sup> develop a trust region framework for managing the use of approximation models in optimization. Chang *et al.*<sup>39</sup> suggest a stochastic trust-region response-surface method. Gano and Renaud<sup>40</sup> introduce a kriging-based scaling function to better approximate the high-fidelity response on a more global level. Rodríguez *et al.*<sup>41</sup> present two sampling strategies, for example, variable and medium fidelity samplings. Jones<sup>42</sup> presents a taxonomy of existing approaches for using response surfaces for global optimization. Other review studies in this field include Sobieszczanski-Sobieski and Haftka<sup>43</sup>, Kleijnen<sup>44</sup>, Kleijnen *et al.*<sup>45</sup>, and Simpson *et al.*<sup>46</sup> and Chen *et al.*<sup>47</sup>.

### 3. Proposed methodology

This section presents the detailed elements of the N-ASRSM. We start the section with a description of the terminology and assumptions followed by an overview of the methodology. Next, we describe the two core strategies embedded in N-ASRSM: (i) nonparametric approach in Sections 3.1–3.5 and (ii) parametric approach in Section 3.6. Finally, in Section 3.7, we describe how these two strategies are integrated within N-ASRSM.

The definitions and terminology used in the proposed N-ASRSM methodology is shown in Table II. Some of the notation is illustrated in Figure 2 for a three-dimensional factor space with *five* initial experiments in each run.

As in most RSM approaches, the proposed N-ASRSM methodology relies on a number of simplifying assumptions. The extensions due to the relaxation of these assumptions are beyond the scope of this paper and some of these extensions discussed in the conclusion. For the proposed methodology, we consider the following assumptions:

1. *The region of interest contains the real optimum of the function.* We assume that the region of interest is shifted close to the optimum a priori using an efficient method (e.g., steepest descent).
2. *The underlying relation between a single response, and two factors can be represented by a quadratic model.* RSM models are usually employed in a sufficiently small region around the optimal region. As a result, it is quite common in RSM applications to assume that the underlying model can be approximated via a quadratic function. Such assumption also holds for this study.
3. *The factor space in the region of interest is feasible.*

Figure 3 illustrates the general scheme of the proposed methodology. The procedure is initialized with the region of interest, for example, a factor space which assumed to contain the optimum. For ease of discussion, it will be assumed here that *O* is a minimum, but maximization is directly comparable. The goal is reach to the vicinity of *O* in a finite set of runs (*R*).

**Table II.** Notations and related description used in this study

Notation	Description
$FS_r$	Factor space at run $r$ and expressed as Cartesian product of factor ranges in run $r$
$D$	Design of most current run
$n$	Number of dimensions
$r$	Index of runs, for example, $r = 1, 2, \dots, R$ , where $R$ is the total number of runs
$e$	Index of experiments in a given run, for example, $e = 1, 2, \dots, E$ , where $E$ is the total number of experiments
$B$	The experiment with the best response level in a given run
$N_k$	The experiment with the $k$ th best response level in a given run ( $2 \leq k \leq E - 1$ )
$W$	The experiment with the worst response level in a given run
$OR_r$	Optimal region in run $r$ containing the estimated optimal experiment, $OR_r, FS_r$
$NOR$	Nonoptimal region
$O$	Optimal experiment, for example, best experiment in the initial factor space
$EO_r$	Estimated optimal experiment in run $r$ , for example, best incumbent estimation of the optimal experiment
$sb$	Index of subregions in a given factor, where the total number of subregions is $2^n$
$c$	Minimum number of required points to estimate quadratic regression parameters ( $c = (n^2 + 3n + 4)/2$ )
$P_i$	Probability of incorrect elimination of $OR$ using ranking strategy
$\alpha$	Bound on the error of incorrect elimination of $OR$

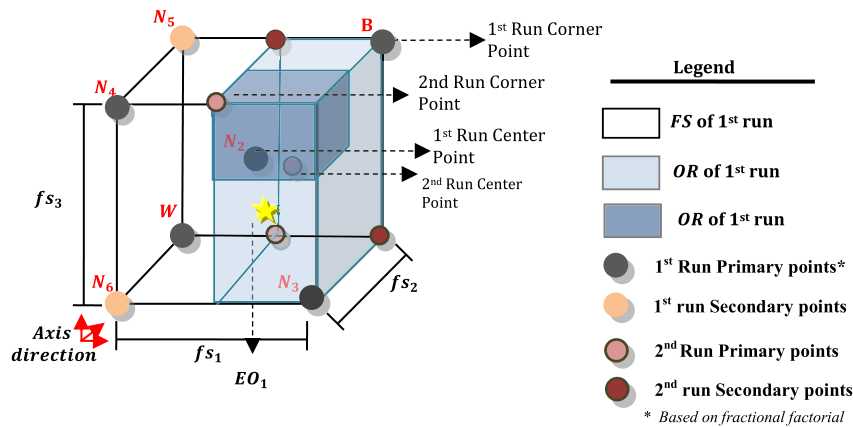


**Figure 2.** An illustration of terminology on a three-dimensional factor space

Each run is setup with a modified version of the factorial design augmented with a center point. Once the experimentation is completed, the approach follows two concurrent strategies, for example, nonparametric ranking strategy and parametric model fitting strategy. Based on the ranking of experiments and the estimated optimal point from quadratic model fitting, a reduced factor space containing the estimated optimal experiment is determined for the next run. This procedure continues until the convergence criteria based on estimated optimal experiment or coefficient of determination of the fitted model is attained. The justification for the dual strategy is that, whereas the information from ranking strategy is accurate but not precise, the information from model fitting is precise but not accurate.

### 3.1. Design structure of the first and subsequent runs

The design  $D$  structure of the factor space  $FS_r$  in the proposed approach is adapted from the minimum resolution fractional factorial design augmented with a center point. This design may be further augmented with few more experiments on the empty corners of  $FS_r$ , which will be discussed in Section 3.6. The justification for choosing the location of the experiments based on fractional factorial design with a center point is that according to Walters *et al.*<sup>48</sup> none of the existing methods for setting the initial point in sequential optimization procedures is superior to the corner point as in fractional factorial design. On the other hand, central points are essential for modeling the curvature of the underlying function.<sup>9</sup>

The factor space of each run ( $FS_r$ ) in the proposed approach can be expressed as a mapping ( $\varphi_r$ ) of the factor space of the preceding run ( $FS_{r-1}$ ) maintaining similar design structure. In most general form, the proposed methodology generates a series of factor spaces, which are nested, for example,  $FS_r = \varphi_r(\varphi_{r-1}(\dots \varphi_0(FS_1)))$ . The output of this mapping  $\varphi_r$  depends on the current factor space, the experimentation design ( $D$ ), the outcome of ranking of experiments as well as the result of parametric strategy described in the next subsection. The latter two, the ranking and the parametric strategies, are described in Sections 3.4–3.7, respectively.

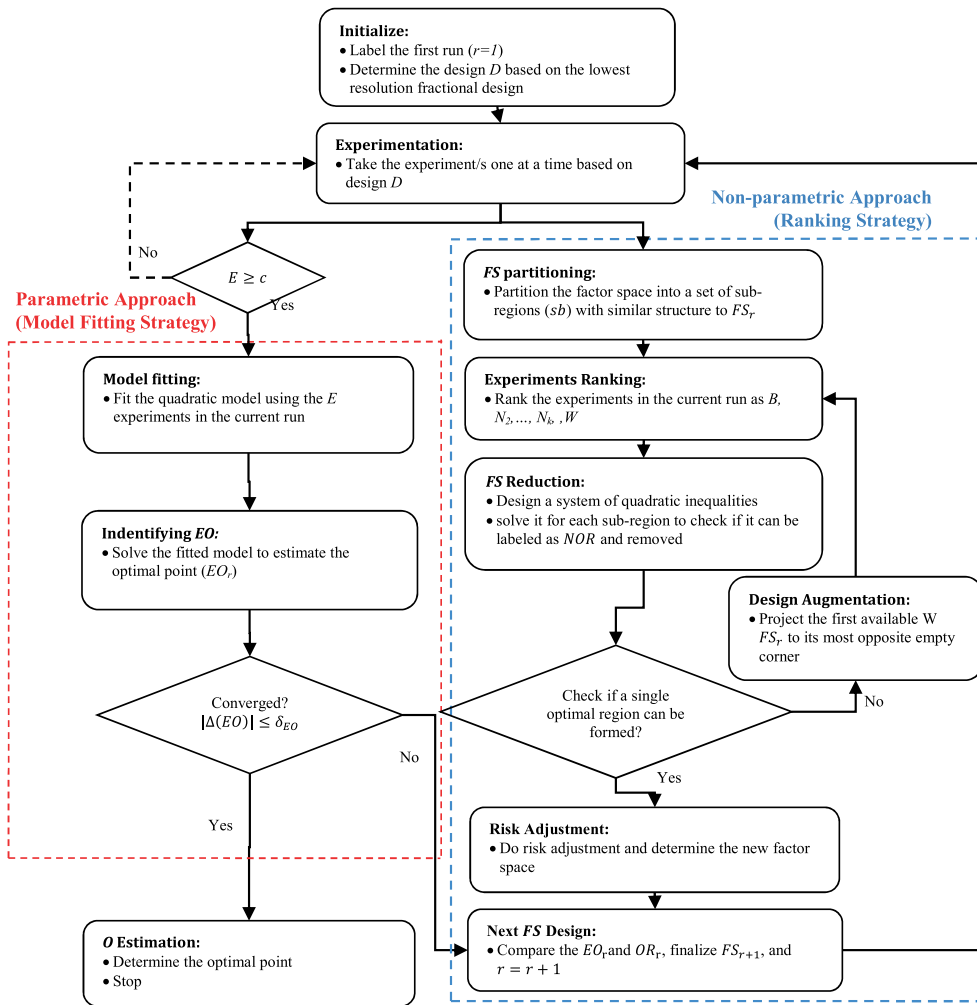


Figure 3. The general scheme of  $n$ -dimensional adaptive sequential response surface methodology

Regarding the  $FS$  size, given that we usually code/normalize factors (variables) in response surface optimization, in the traditional CCD and BBD approached, the corner points are taken at  $\pm 1$  unit distance from the center point (0,0). In contrast, in the proposed methodology, it is suggested to start with a broader initial region around the center point in comparison with the classic approached, for example,  $\pm 2^{\frac{n-f}{4}}$  unit distance from the center where  $2^{n-f}$  the number of points is in the chosen fractional factorial design (above relation is based on the calculation axial points in rotatable CCD with a single replicate at all designated points.<sup>9</sup> Although beginning with a larger space is initially disadvantageous, experimental results demonstrate that the reduction in the factor space with the same number of experiments far exceeds initial difference. An additional benefit is that this modification may decrease the effect of random error on the initial results. Let's consider the diagonal cross section of these two designs in at one dimension as illustrated in Figure 4 (b) and assume that the noise is identically distributed on this cross section. Then, it can be shown that the impact of the noise on prediction of the optimal experiment point is less with the proposed methodology's factor space. Figure 4 compares the initial factor space of the traditional CCD and the proposed.

### 3.2. Nonparametric approach: ranking strategy

At each run  $r$  of the proposed N-ASRSM approach, we first rank the experiments (e.g.,  $k$ th point fractional factorial and one center points) as  $N_1$  (we would call  $B$ ),  $N_2 \dots, N(k-1)$  and  $N(k-1)$  (we would call  $W$ ) according to their response levels. The experiment called  $B$  is the best location observed so far and  $W$  is the worst location observed since the goal is to minimize the response. Based on the ranking, we identify the implied optimal region, which contains the  $EO_r$ . This region is a polygon contained in  $FS_r$ , and can be convex or nonconvex in the space of factors. We then identify a hyper rectangle, which contains the implied optimal region and denote it as the optimal region ( $OR_r$ ), which determines the factor space of the next run.

This process of encapsulating the implied optimal region with a hyper rectangle is a form of relaxation and is not efficient in terms of factor space reduction. However, there are valid reasons, which motivate this relaxation. The foremost reason is the reduced need for new experiments due to the inheritance of experiments from the previous run. Secondly, the hyper-rectangular  $FS$  preserves the orthogonality of factorial experimental design. Further, this hyper-rectangular form facilitates the recursive characterization of the

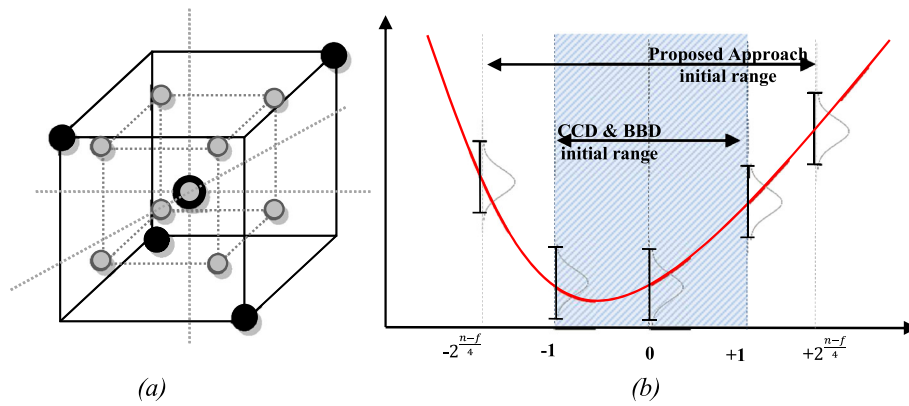


**Figure 4.** (a) Initial factor space and design structure and (b) diagonal cross-section of the traditional central composite design and proposed  $n$ -dimensional adaptive sequential response surface methodology approach.

same rectangular structure throughout the process. In addition, we can use the same experimental design structure, for example, factorial with a center point. Specifically, with hyper-rectangular envelope, the mapping across runs will be identical, for example,  $\varphi(\cdot)$   $\varphi_r(\cdot)$  for  $\forall r$ . This is because we maintain the same experiment design structure, and there is a finite number of estimated optimal region through different runs as a result of ranking outcomes. Lastly, the relaxation reduces the risk of selecting an optimal region, which excludes the optimal experiment.

An alternative to the hyper-rectangular envelope is the convex hull of implied optimal region. Due to its convexity, it also allows for easier tessellation of the  $FS$ . Although the convex hull reduces the optimal region more than the hyper-rectangular envelope, it does not reduce the number of new experiments as much. Furthermore, the experimental design used in each run will be different because the convex hulls of the implied optimal regions will vary in shape. Clearly the choice of the right form is a trade-off between the rate of contraction of the optimal region and the total number of experiments conducted.

To better illustrate this trade-off, let's consider the implied optimal region in Figure 5(a). The convex hull of this implied optimal region is identified in Figure 5(b) with 10 vertices (corner points). In contrast, we adopted the rectangular envelope, which is illustrated in Figure 5(c). Comparison between Figure 5(b) and (c) reveals that, while convex hull-based optimal region (OR) leads to the greatest factor space reduction, it also leads to an increased number of new experiments (10 vs. 7 corners for new experiments). In other words, in Figure 5, the implied OR in (b) is smaller than the rectangular envelope in (c), hence the reduction is more in (b); but this does not facilitate the re-use of previous points in the next iteration, hence we compromise the efficiency in region reduction with the efficiency of eliminating the need to take new points.

In what follows, we first present the methodology used to reduce the factor space. Next, we describe how to choose additional experiments for characterizing a hyper-rectangle OR (last step in the nonparametric approach part of the algorithm).

### 3.3. Reducing factor space

The reduction of the factor space to a subregion containing  $O$  is achieved through the ranking of experiments of the current run. This reduction is performed by elimination of those subregions that do not contain the optimal point, for example, nonoptimal regions (NOR). The determination of such subregions would be exact if there were no noise and the assumptions stated in Section 3.1 held. In the presence of noise and deviations from the quadratic model, it is approximate. Intuitively, the subregions in the vicinity of high and low ranking experiments are more simply characterized as a NOR or OR. In particular, the vicinity of  $B$  has a higher probability of

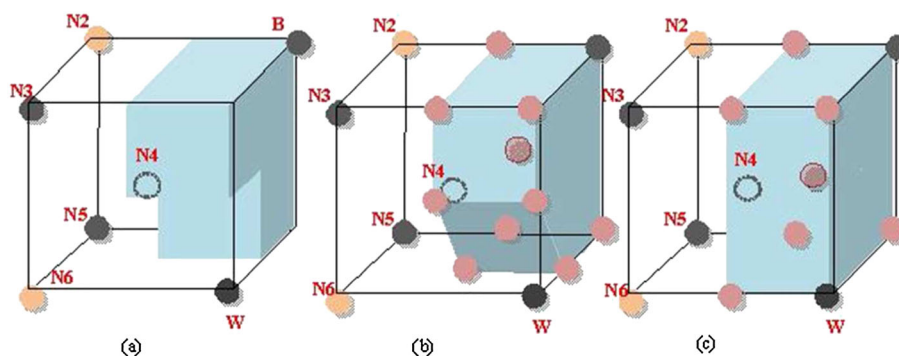


**Figure 5.** (a) Implied optimal region, (b) convex hull envelope of the implied optimal region, and (c) rectangular envelope of the implied optimal region

containing  $O$ , whereas the other regions, for example, the vicinity of  $W$ , have considerably less chance of containing  $O$ . Such confidence decreases in the vicinity of less extreme points. This intuition can be formalized in a procedure as follows:

**Procedure 1**

NORs elimination

- Step 1. Divide  $FS$  into  $2^n$  subregions of the same size and structure by bisecting the  $FS$  using  $n$  hyperplanes orthogonal to the each  $n$  factors (dimensions) (Figure 6(a)).
- Step 2. For each of the  $2^n$  subregions, repeat:
  - 2.1. Identify a hypothetical optimal point  $\hat{O}$  in the current subregion (Figure 6(b)).
  - 2.2. For each experiment  $1 \leq e \leq E$ , express the response model in a canonical form as  $Z_e = \sum_{i,j=1}^n A_{i,j} (X_i^e - X_i^{\hat{O}}) (X_j^e - X_j^{\hat{O}}) + R$ , where  $A_{i,j} \in R$  and  $R$  is a constant term (Figure 6(c)).
  - 2.3. Sort the parametric canonical forms of the experiments in ascending order ( $Z_{e_B} < Z_{e_{N_2}} < \dots < Z_{e_W}$ ). (Because the canonical form should comply with empirical ranks of the experiments ( $B < N_2 < \dots < N_k < W$ ). (Figure 6(d))
  - 2.4. Rewrite the sorted canonical forms of the experiments in the form of a system of inequalities with  $\frac{E(E-1)}{2}$  pairwise comparisons of experiments as follows (Figure 6(e)):

$$\begin{cases} Z_{e_B} - Z_{e_{N_2}} = \sum_{i,j=1}^n A_{i,j} (X_i^{e_B} - X_i^{\hat{O}}) (X_j^{e_B} - X_j^{\hat{O}}) - \sum_{i,j=1}^n A_{i,j} (X_i^{e_{N_2}} - X_i^{\hat{O}}) (X_j^{e_{N_2}} - X_j^{\hat{O}}) < 0 \\ Z_{e_{N_2}} - Z_{e_{N_3}} = \sum_{i,j=1}^n A_{i,j} (X_i^{e_{N_2}} - X_i^{\hat{O}}) (X_j^{e_{N_2}} - X_j^{\hat{O}}) - \sum_{i,j=1}^n A_{i,j} (X_i^{e_{N_3}} - X_i^{\hat{O}}) (X_j^{e_{N_3}} - X_j^{\hat{O}}) < 0 \\ Z_{e_{N_k}} - Z_{e_W} = \sum_{i,j=1}^n A_{i,j} (X_i^{e_{N_k}} - X_i^{\hat{O}}) (X_j^{e_{N_k}} - X_j^{\hat{O}}) - \sum_{i,j=1}^n A_{i,j} (X_i^{e_W} - X_i^{\hat{O}}) (X_j^{e_W} - X_j^{\hat{O}}) < 0 \end{cases} \quad (2)$$

(In the previous system  $A_{i,j}$  and  $X_j^{\hat{O}}$  are the unknowns, where  $X_j^{\hat{O}}$  is bounded by the borders of the current subregions)

- 2.5. Check the feasibility of the previous system by looking for a negative solution of the following Max–Min optimization model: (Figure 6(f))

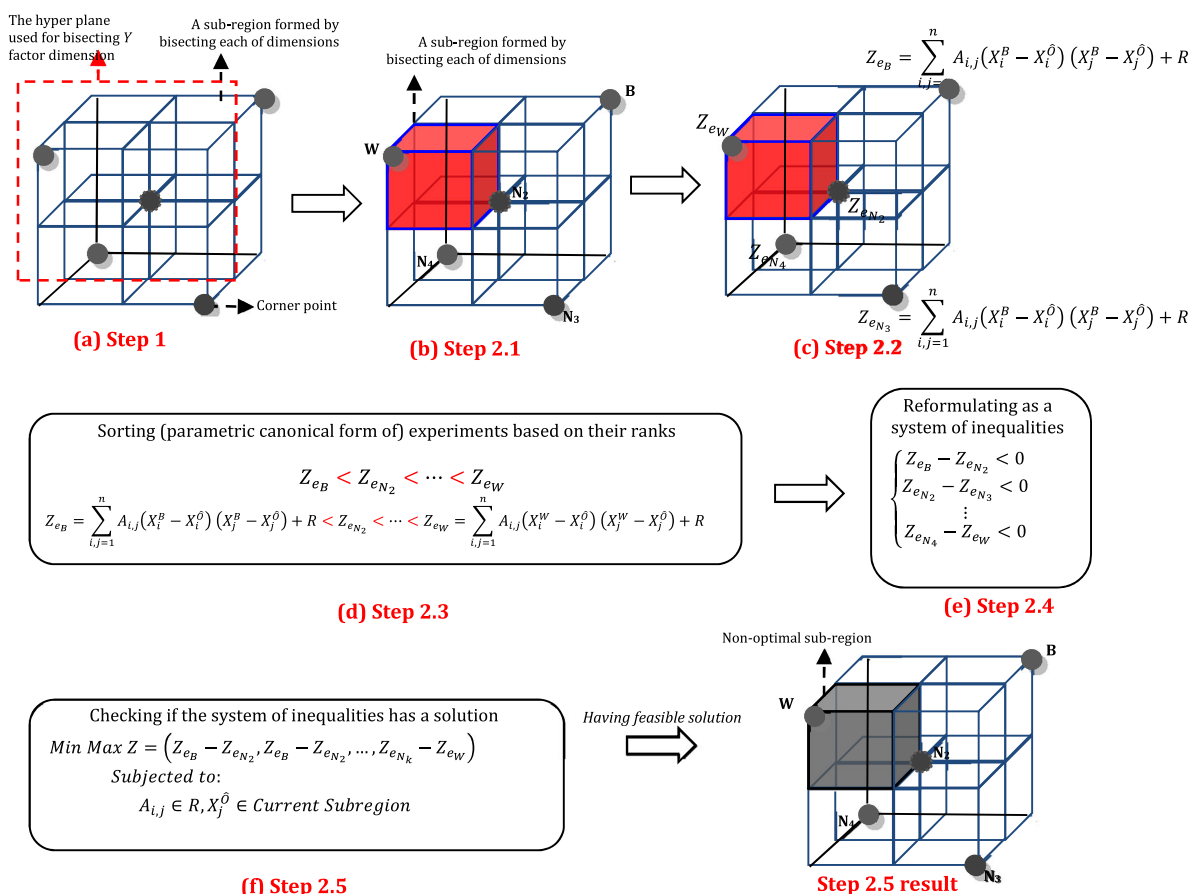


**Figure 6.** Graphical representation of step 1 and 2 of the nonoptimal regions elimination algorithm on a sample three-dimensional factor space

$$\begin{aligned} \text{Min Max } Z &= (Z_{e_B} - Z_{e_{N_2}}, Z_{e_B} - Z_{e_{N_2}}, \dots, Z_{e_{N_k}} - Z_{e_W}) \\ \text{Subjected to :} & \\ A_{i,j} \in R, X_j^{\hat{O}} &\in \text{Current Subregion} \end{aligned} \quad (3)$$

(Positive solution of previous optimization model is equivalent to nonexistence of a feasible solution for previous system of quadratic inequalities and vice versa; Figure 6(f)).

Feasible solution of previous system of quadratic inequalities in (2) simply means the real optima ( $O$ ) can occur in the subregion stated by step 2.1, otherwise that subregion is not feasible and can be eliminated from the OR. It can be shown that the previous procedure eliminates only those subregions not containing the optimal point by contradiction as per the assumptions stated in Section 3.1. In particular, we first assume that there exists a subregion containing the optimal point, which leads to an inconsistent ranking of at least one experiment pair. Next, we show that the  $A_{i,j=1,\dots,n}$  determined for the experiment pair contradicts the convexity assumption of the quadratic response forms. It should be noted that the main reason for using the canonical form of response models in step 2.2 of previous procedure is to reduce the number of parameters to be estimated.

The NOR elimination steps are repeated for all subregions until those subregions not eliminated or not checked form a hyper-rectangular region inside the FS. When such a hyper-rectangular region is obtainable, we then designate it as the FS of the next run. Appendix B provides an estimate of NOR reduction rate of nonparametric approach for different number of dimensions (number of variables). The computational complexity of nonparametric approach is also discussed in Appendix C. If a hyper-rectangular region is not available upon the checking of all subregions for NOR elimination, then additional corner experiments are necessary. The next section discusses how those additional experiments are determined.

### 3.4. Design augmentation: selecting additional corner points

When the NOR elimination procedure terminates without a candidate hyper-rectangular FS or very small eliminated subregion, then additional points are needed. These additional points enable eliminating more of the subregions in a few ways. First, they increase the number of pairwise-ranking comparisons of experiments such that the likelihood of a previously noneliminated subregion becoming a NOR is increased. Second, with these additional points, the new ranking of the experiments leads to a better coverage of FS. Finally additional points generally result in more reliable ranking of the experiments that potentially allow elimination of more subregions. However, because one of the goals of N-ASRSM is to reduce the total number of experiments, the number of additional points should be kept as small as possible. This can be achieved by selecting the additional points that provide maximum potential for eliminating NORs.

We select additional points one at a time until the next FS as a hyper-rectangle can be inferred. The selection strategy employed is based on the simplex optimization method in Walters *et al.*<sup>48</sup> and aims at maximizing the potential of eliminating more NORs. This strategy is executed by using the current ranking information of the experiments and subsequently identifying those directions with most improvement of response based on the current experiments. Clearly, the lowest ranking experiment ( $W$ ) is an ideal candidate for identifying such direction for two reasons. First, the most opposite corner projection of  $W$  provides valuable information on the orientation of the diagonals of the underlying function. The second reason is, as in the simplex optimization method, the projection in the opposite of least favorable ( $W$ ), is likely to produce a new ranking with a more precise range of response orientation. Once the opposite projection of  $W$  is taken as additional points, we continue taking additional points in the opposite reflections of next low-ranking experiment, for example,  $N_{E-2}$  and  $N_{E-3}$ , and so on. Figure 7 illustrates an example of two additional points taken in a three dimensional FS as the opposite projections of first  $W$  and then  $N_5$ .

The most opposite projection of an experiment is determined according to the cosine similarity measure.<sup>49</sup> To illustrate, the most opposite corner projection of the worst experiment  $W$  can be found by:

$$C_k = \arg \min_{C_k} \cos(\alpha) \quad (4)$$

where  $\alpha$  is the angle between  $C_w$  and  $C_k$ ; vectors connecting and the candidate empty corner to the center point (projection of  $B$  can be carried out in the same way). Previous procedure works while the candidate experiment is a corner points. If the candidate experiment, for example,  $W$ , happens to be a center point, then opposite projection of the next candidate experiment, for example,  $N_{E-1}$ , should be considered.

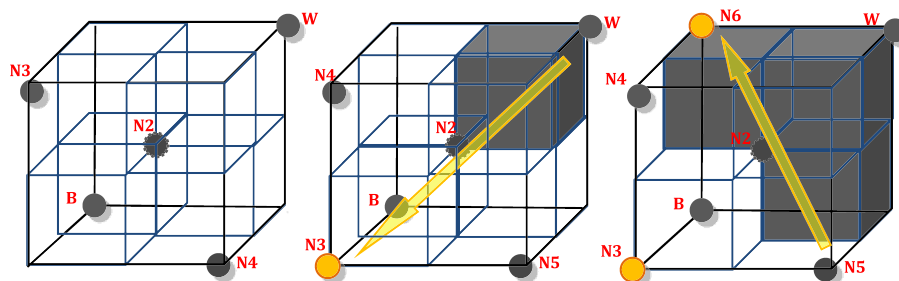


Figure 7. An example of eliminating nonoptimal regions in a three-dimensional factor space using the ranking strategy based on two additional points

### 3.5. Risk adjustment

Reducing factor space is exact when there is no noise; however, when the data have error, there is some probability that two or more of the rankings are incorrect and the selected feasible region may be inaccurate (Figure 8).

Knowing the probability of incorrectly ranking the experiments can help to change the size of the *OR* to adjust the risk of not containing the *O*. The challenge is that the variance of the noise is unknown and the number of experiments is usually not enough (especially in the early runs) to estimate the variance. In the rest of this section, we present a novel approach for finding a (pessimistic) estimate of variance when there is not enough data to estimate the model parameters and suggest how this might be used to reduce the risk of not containing the *O* in *OR*.

**3.5.1. Estimating the variance with insufficient data** When the number of experiments is not enough to estimate all parameters of the model, we design a system of two equations for obtaining the pessimistic estimate of variance. The first equation decomposes total sum of square (*SST*) into sum of square regression (*SSR*) and sum of square error (*SSE*):

$$SST = SSE + SSR \quad (5)$$

The second equation is derived based on minimum significance level of the meaningfulness of the regression of the hypothesis testing regression analysis. The test statistic is  $F = \frac{SSR/k-1}{SSE/n-k}$ , where  $k$  is the number of parameters in the canonical form of response model discussed in Section 3.5 and is the total number of experiments. The main reason for using the canonical form of the response model for calculating  $k$  is to reduce the number of parameters to be estimated; because we assume *O* is known, canonical modeling can reduce the number of parameters to be estimated. The critical value of the hypothesis test is  $F_{\alpha,k-1,n-k}$ , so at the significance level  $\alpha$  considering the minimum value of the statistics, which makes the regression meaningful the following equation can be written as:

$$\frac{SSR}{k-1} - F_{\alpha,k-1,n-k} \cdot \frac{SSE}{n-k} = 0 \quad (6)$$

In (5) and (6), *SST*,  $k-1$ ,  $n-k$ , and  $F_{\alpha,k-1,n-k}$  are known and *SSR* and *SSE* are unknown, so combining (5) and (6) will result in a system of two equations and two unknowns. One of the solutions of previous system would be *SSE*, which can be used for estimating the variance through Mean Squared Error (*MSE*) ( $\hat{V}ar = MSE = \frac{SSE}{n-k}$ ). Of course, if there is sufficient data or replications are made, a more traditional estimate of *MSE* should be used. With a bound on the error, error in ranking the design points can be considered and used to properly determine how to expand the *OR* to account for these errors. Next section provides an intuitive procedure for risk adjustment of *NOR* using *MSE*.

**3.5.2. An intuitive method for nonoptimal region risk adjustment** Having *E* ranked experiments in a way that  $e_1$  to  $e_E$  represents *B* to *W*, respectively, using the (pessimistic) estimate of variance from Section 3.5.1, for each pair of experiments  $(e_i, e_j)$ , ( $i < j$ ) the probability of incorrect ranking can be approximated using normal density function:

$$p(e_j < e_i) = \varphi\left(\frac{Z_{e_i} - Z_{e_j}}{\sqrt{2MSE}}\right) \quad (7)$$

where  $Z_{e_i}$  and  $Z_{e_j}$  are the observed values for experiments  $e_i$  and  $e_j$ , *MSE* is the (pessimistic) estimate of variance, and  $\varphi$  is the cumulative density function of standard normal distribution. The following procedure incorporates Equation (7) to formalize an algorithm for estimating the probability of incorrect elimination of *OR*:

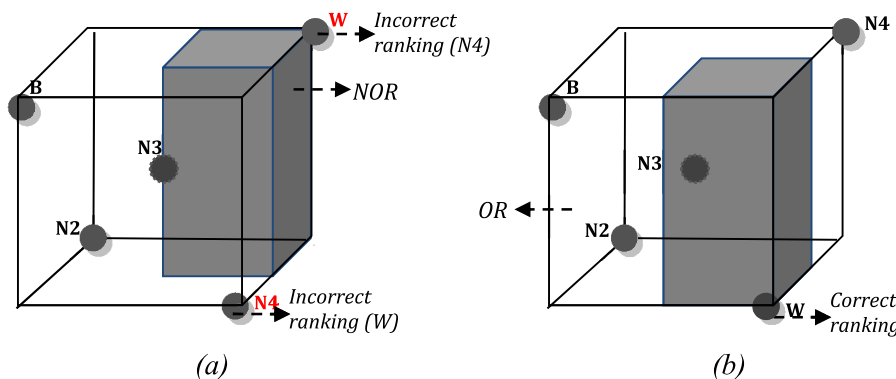


**Figure 8.** An example of the effect of incorrect ranking on the nonoptimal region: (a) nonoptimal region identified on the basis of noisy data (incorrect ranking of *W* and *N4*), (b) nonoptimal region identified on the basis of noise free (correct ranking)

**Procedure 2**

For estimation the probability of incorrect elimination of OR

- Step 1. Set  $r = 1$ .
- Step 2. For each experiments,  $e_i \in \{e_1, \dots, e_E\}$  change the rank with the next inferior experiments ( $e_i \leftrightarrow e_{i+1}$ ).
- Step 3. If changing the ranks modifies NORs, find the probability of incorrect ranking using (7) and go to step 4. Otherwise go to step 5.
- Step 4. From all possible rank changes, which result in modification of NORs (in step 3), find the one with maximum probability of incorrect ranking ( $P_i$ ) as the estimated probability of incorrect elimination of OR
- Step 5. Set  $r = r + 1$  and go to step 2

The previous procedure is based on OFAT analysis and has computational complexity of  $O(n)$ . Nonetheless, it has shown good performance comparing to exhaustive search with  $O(n^2)$  complexity in the numerical examples we conducted.

Procedure 2 states that when data are noisy, there is a risk of  $P_i$  in the elimination of NORs from FS using ranking strategy. And that is the risk of incorrect elimination of OR instead of NOR (Figure 9). It is also clear that there is no risk in no elimination (keeping NOR). Therefore, with a bound on the error of incorrect elimination of  $R(\alpha)$ , the correct rate of reduction in NOR (PR), that is, expansion in OR, which account for risk of incorrect elimination of OR can be approximated by solving the logistic function<sup>50</sup> shown in Equation (8) for  $Y(PR) = \alpha$ , which results in the PR (Percent of Reduction) value presented in (9):

$$Y(PR) = \frac{P_i}{(1 + e^{-(B_0 + B_1 \cdot PR)})} \tag{8}$$

$$PR = \frac{\ln(\alpha / (P_i - \alpha)) - B_0}{B_1} \tag{9}$$

In Equations (8) and (9),  $B_0$  and  $B_1$  are the shape parameters of the function. These parameters are chosen to limit the function range to (0,1) (in this study, we use  $B_0 = 10$  and  $B_1 = 100$ ). The main reason for using the generalized logistic function (instead a typical logistic function) is the extra shape parameter, which provides additional flexibility. Figure 9 illustrates how the generalized logistic function applies to NOR reduction.

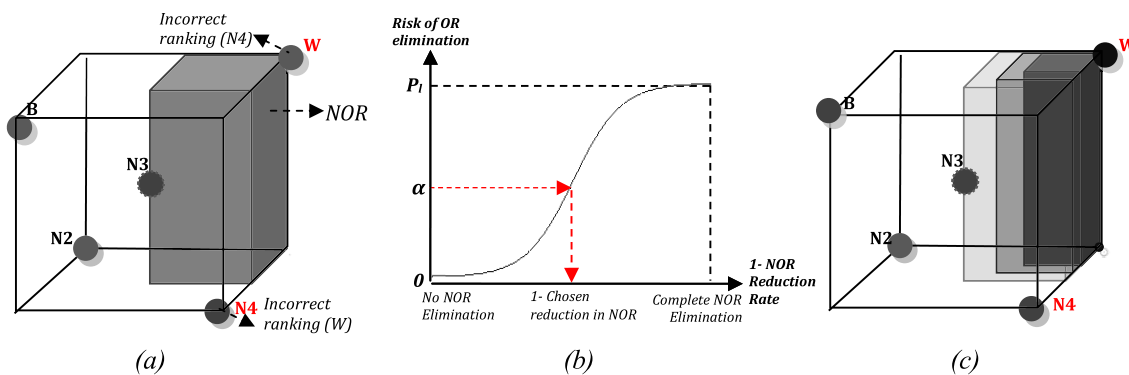


**Figure 9.** Application of the generalized logistic function nonoptimal region risk adjustment: (a) nonoptimal region identified on the basis of noisy data, (b) the generalized logistic function with specified  $\alpha$  and related PR rate, and (c) the effect of different values of PR on the size of nonoptimal region

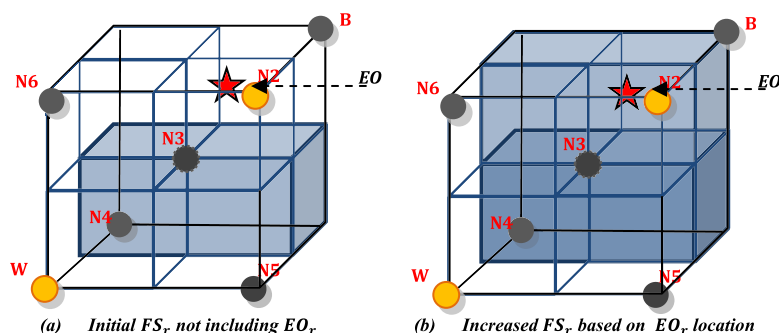


**Figure 10.** Expansion of optimal region when the estimated optima  $EO$  falls outside

### 3.6. Parametric approach: model fitting strategy

We use a parametric approach based for model fitting concurrent to the nonparametric ranking approach described in Section 3.4. This strategy not only allows us to increase the precision of  $EO_r$ , but also supports backtracking through the expansion of  $OR_r$  to contain estimated optimal  $EO_r$ . Beginning with the completion of all first run experiments, this parametric approach is used after each experiment. In this approach, we fit a quadratic model:  $Z = \sum_{i,j=1}^n Q_{ij}x_i x_j + \sum_{i=1}^n P_i x_i + R + \varepsilon$ , with  $\varepsilon \sim N(0, \sigma^2)$ , to the experimental data to analyze the underlying function and efficacy of conducted experiments. In fitting the quadratic model, two objectives are being sought in particular: (i) finding the estimated optimal experiment ( $EO_r$ ); and (ii) calculating the adjusted coefficient of determination ( $R_{adj}^2$ ).  $EO_r$ , the minimum of the fitted model, not only shows the predicted optimal solution but also used for the expansion of  $OR_r$ . Furthermore, the change in the  $EO_r$  in consecutive runs is also used as a stopping criterion.  $R_{adj}^2$  shows how well the information gained from the experiments explain the behavior of the underlying system.<sup>51</sup> This measure can be used as an additional stopping rule in the proposed N-ASRSM methodology.

### 3.7. Designing next run factor space: expansion of optimal region to contain estimated optimal

As described in the N-ASRSM algorithm in Section 3.2, we check the consistency of the  $EO_r$  obtained from the parametric approach and the estimated optimal region  $OR_r$  obtained from the nonparametric strategy. When the  $EO_r$  is found to be outside  $OR_r$ , we then expand the  $OR_r$  to contain  $EO_r$ , while preserving its hyper-rectangular structure. The resulted region will then be used as the FS of the next runs. This expansion is illustrated in Figure 10.

## 4. Simulated experiments and case studies

In this section, we first illustrate the results of a rat brain trauma case study comparing the proposed N-ASRSM and tradition CCD approach. Next, we report on the results of two sets of extensive simulation experiments performed to evaluate the performance

**Table III.** The experiments of the brain trauma case study: (a) central composite design and (b)  $n$ -dimensional adaptive sequential response surface methodology

Experiment no. (Exp no.)	Controllable factors/impact parameter (coded)				Random factor	Response		Experiment no. (Exp. no)
	Impact depth	Impactor diameter	Impact velocity	Impactor shape	Brain size variation (%)	Brain injury	Run	
1	-1	-1	-1	-1	0	694.95	1	1
2	1	-1	-1	-1	1	3.46		2
3	-1	1	-1	-1	-2	281.96		3
4	1	1	-1	-1	0	46306.31		4
5	-1	-1	1	-1	1	58.49		5
6	1	-1	1	-1	1	1462.11		6
7	-1	1	1	-1	1	1500.08		7
8	1	1	1	-1	0	77150.12		8
9	-1	-1	-1	1	0	822.78		9
10	1	-1	-1	1	-1	823.36		10
11	-1	1	-1	1	1	699.20		11
12	1	1	-1	1	2	327.05		12
13	-1	-1	1	1	-2	537.74		13
14	1	-1	1	1	1	793.37		14
15	-1	1	1	1	0	3.03		15
16	1	1	1	1	0	7313.50		16
17	-2	0	0	0	1	900.00	2	1 (17)
18	2	0	0	0	0	13452.45		2 (18)
19	0	-2	0	0	1	102.94		3 (19)
20	0	2	0	0	-2	8112.84		4 (20)
21	0	0	-2	0	0	448.04		5 (21)
22	0	0	2	0	1	2468.18		6 (22)
23	0	0	0	-2	-1	5139.05		
24	0	0	0	2	0	6.19		
25	0	0	0	0	0	145.26		

N/A: not applicable.

of the proposed N-ASRSM approach. In the first set of simulations N-ASRSM is compared with well-known classical methods including CCD, BBD, and A-optimal, D-optimal, and V-optimal designs on different quadratic response models with varying variance of errors. The second set of simulations study the performance of the proposed approach along with classical models, optimal designs, optimal adaptive sequential response surface methodology (O-ASRSM) method,<sup>33</sup> and four global optimization methods including: Standler *et al.*<sup>29</sup>, Wang *et al.*<sup>28</sup>, EGO,<sup>37</sup> a radial basis function (RBF) method<sup>52</sup> on a number of nonlinear response models with various errors.

#### 4.1. Traumatic brain injury: design of controlled cortical impact model

Traumatic brain injury (TBI) continues to be a serious societal problem that affects 1.7 million Americans each year.<sup>53</sup> In the European Union, brain injury accounts for 1 million hospital admissions per year.<sup>54</sup> Fatality due to TBI can occur in children and adults during their most productive years, and the associated society and economic costs are enormous. Direct medical cost and indirect costs such as lost productivity of TBI totaled an estimated \$60 billion in the USA in 2000. Additionally, there are many survivors with severe brain damage and many more with moderate or mild impairment, which require continuous medical attention.<sup>53,55</sup>

Controlled cortical impact (CCI) is one of the mostly used laboratory TBI experiments for studying mechanisms and treatment of brain injuries using rodent subjects (e.g., 8, 9, 10). Briefly, to induce CCI injuries, a craniotomy was performed over the skull and a metal tip was driven to compress exposed dural tissue to a predefined depth at controlled velocity. As summarized from 235 papers on CCI, various impact depths, impact velocities, impactor sizes, and impactor shapes were used by different laboratories to have desired brain injury.<sup>56</sup> Numerical analysis was adopted to systematically analyze how external impact parameters (such as depth and velocity) affect brain injury intensity<sup>56</sup> finding that impact depth was the leading factor followed by, surprisingly, impactor shape, which was not fully considered by experimentalists. Furthermore, the effect of CCI parameters on regional injury intensity at different components was numerically analyzed. All these numerical studies provide guidance to have desired injury level by carefully assembling different external parameters. Still, an efficient methodology is needed given the complexity of CCI experiments, which are not only expensive but also very time consuming.

**4.1.1. Method selection** The range of impact parameters were defined based on the range of laboratory CCI experiments,<sup>56</sup> ranging from mild to severe brain injuries. The impact depth ranged from 0.7 mm to 3.0 mm. The impactor diameter ranged from 1.8 mm to 7.5 mm. The impact velocity ranged from 2 m/s to 7 m/s. The impactor shape was also continuously varied, with 0 representing pure flat shape and 1 representing hemispherical shape. All CCI simulations were performed using LS-DYNA MPP 971 (LSTC, Livermore, CA). The percent of increase/decrease in size of rat brain, which contributes to variances observed in post-impact tissues is considered as noise; because typically the effect of this external parameter is largely unknown. An in-house written program was used to calculate the volume of elements, which experienced maximum principal strains above 0.3 during the whole simulation. In other word, the objective of the case study is to find the specific levels of the impact parameter that result in 30% of injury in animal brain.

Controllable factors/impact parameter (coded)				Random factor	Response	
Impact depth	Impactor diameter	Impact velocity	Impactor shape	Brain size variation (%)	Brain injury	Percent of FS reduction (before risk adjustment; %)
-2	-2	-2	-2	1	900.00	N/A
2	-2	-2	2	2	682.18	N/A
-2	2	-2	2	-1	900.00	N/A
2	2	-2	-2	1	58,407.63	N/A
-2	-2	2	2	0	889.19	N/A
2	-2	2	-2	1	3,610.40	N/A
-2	2	2	-2	1	4,250.04	N/A
2	2	2	2	2	170,415.48	N/A
0	0	0	0	-1	130.66	0
0	-2	0	0	1	102.94	0
0	2	0	0	-2	8,112.84	0
-2	-2	-2	2	-1	900.00	0
2	2	-2	2	2	35,088.07	6
-2	0	0	0	1	900.00	6
-2	2	2	2	0	705.72	6
-2	2	-2	-2	-1	811.66	44
1	-1	-1	-1	1	3.46	63
-1	1	-1	-1	-2	281.96	44
-1	-1	1	-1	1	58.49	44
1	1	1	-1	0	77150.12	69
-1	-1	-1	1	0	822.78	81
1	1	-1	1	2	327.05	≈100

In this case study, we used the proposed approach along to find the parameter setting that result in 30% injury in the rat brain. We also conducted CCD experiments to compare the performance with the proposed approach. More technical details of the experiments can be found in Mao *et al.*<sup>55</sup>. Table III(a) and (b) shows the conducted experiments of CCD along with the percent of change in the rat brain (comparing with the standard case) and amount injury to the rat brain (the response) due to the impactor. Using Table III(a) data, CCD

**Table IV.** Response models used in the simulated experiments

No. of variables	Exp. no.	Response relation	Error ( $\epsilon$ )	Response type
Two variable response	1.1	$W = x^2 + 2y^2 - 2y + \epsilon$	$N(0,1)$	Convex
	1.2	$W = -2x^2 + 3y^2 + 2x - y + 2xy - 1 + \epsilon$	$N(0,2)$	Nonconvex
	1.3		$N(0,2)$	Convex
Three variable response	2.1	$W = 2x^2 + 3y^2 + 5z^2 + x + 2y + 1z - 5xy + 1xz + 1yz + 1 + \epsilon$	$N(0,3)$	Convex
	2.2	$W = -1.5x^2 - 3.5y^2 + 3z^2 + 0.5x - 3.5y - 1.5z - 3xy + 1.3xz + 1.4yz + 2 + \epsilon$	$N(0,2.5)$	Nonconvex
Six variable response	3.1	$W = (t - 0.55)^2 + (u + 0.7)^2 + (v - 0.33)^2 + (x - 1.55)^2 + (y + 0.9)^2 + (z - 0.3)^2$	$N(0,1)$	Convex
	3.2	$W = (t - 1.65)^2 + (u + 1.7)^2 + (v - 1.45)^2 + (x - 2.11)^2 + (y + 1.91)^2 + (z - 2.01)^2 + (t - 2)(u - 2.2) + (u - 1.54)(v - 0.02) + (u - 0.34)(z - 2.33) + (v - 0.34)(y - 1.33) + (y - 0.53)(z - .65)$	$N(0,2)$	Convex

**Table V.**  $R^2_{adj}$  for trials 7, 8, and 9 of the responses with two variables; trials 11, 12, and 13 of the responses with three variables; and trials 34, 35, and 36 of the responses with six variables

Exp. no.	Number of observations (No obs.)	Adjusted R <sup>2</sup>						
		CCD (%)	BBD (%)	N-ASRSM (%)	D-Opt. (%)	V-Opt. (%)	A-Opt. (%)	O-ASRSM (%)
1.1	7	92.69	N/A	93.67	95.01	94.85	90.69	<b>98.74</b>
	8	92.48	N/A	95.97	89.20	95.86	86.86	<b>98.42</b>
	9	92.00	N/A	<b>97.94</b>	90.42	95.42	86.58	97.15
1.2	7	69.77	N/A	79.57	92.96	72.11	<b>97.71</b>	92.95
	8	70.60	N/A	89.53	91.06	74.92	79.86	<b>94.59</b>
	9	88.48	N/A	93.91	89.02	80.89	82.00	<b>95.55</b>
1.3	7	35.45	N/A	86.08	85.31	85.08	50.38	<b>86.09</b>
	8	43.17	N/A	<b>86.84</b>	78.71	86.04	57.23	86.78
	9	49.40	N/A	<b>89.95</b>	67.65	82.05	64.49	89.06
Avg.	7	65.97	N/A	86.44	91.09	84.01	79.59	<b>92.59</b>
	8	68.75	N/A	90.78	86.32	85.61	74.65	<b>93.26</b>
	9	76.63	N/A	<b>93.93</b>	82.36	86.12	77.69	93.92
2.1	11	80.64	79.93	91.44	94.33	<b>97.16</b>	87.40	92.42
	12	86.42	81.86	<b>93.40</b>	93.39	81.34	90.36	92.81
	13	86.93	81.16	<b>95.48</b>	94.03	77.13	88.66	93.78
2.2	11	89.02	53.12	<b>99.38</b>	89.25	84.88	90.50	98.39
	12	87.06	56.04	94.99	92.93	86.88	91.76	<b>97.37</b>
	13	86.50	49.48	94.27	91.74	88.27	90.12	<b>95.36</b>
Avg.	11	84.83	66.53	<b>95.41</b>	91.79	91.02	88.95	<b>95.41</b>
	12	86.74	68.95	94.20	93.16	84.11	91.06	<b>95.09</b>
	13	86.72	65.32	<b>94.88</b>	92.89	82.70	89.39	94.57
3.1	34	80.21	70.00	94.61	90.20	<b>96.49</b>	90.20	98.63
	35	79.61	70.10	99.83	91.84	96.76	91.84	<b>98.94</b>
	36	79.82	64.18	<b>99.83</b>	92.73	97.26	92.73	99.05
3.2	34	99.56	98.27	99.50	97.80	<b>99.93</b>	99.82	99.92
	35	99.55	98.27	<b>99.94</b>	99.81	<b>99.94</b>	99.85	<b>99.94</b>
	36	99.55	98.27	<b>99.96</b>	99.82	99.94	99.81	99.95
Avg.	34	89.89	84.14	97.06	94.00	98.21	95.01	<b>99.28</b>
	35	89.58	84.19	<b>99.89</b>	95.83	98.35	95.85	99.44
	36	89.69	81.23	<b>99.90</b>	96.28	98.60	96.27	99.50

Avg.: average; CCD: central composite design; BBD: Box-Behnken design; N-ASRSM: *n*-dimensional adaptive sequential response surface methodology; D-Opt.: D-optimal; V-Opt.: V-optimal; A-Opt.: A-optimal; O-ASRSM: optimal adaptive sequential response surface methodology; N/A: not applicable.

estimate fit a quadratic regression with  $R^2_{adj} = 45.63$  and the estimated optimal impactor setting of  $EO = [-1.88, -2.00, 1.88, -2.00]$  (Also see the fitted quadratic surfaces of CCD in A.1). Table III(b) also illustrates the conducted experiments of proposed N-ASRSM method along with the percent of reduction in the factor space after each additional experiment. As can be seen from Table III(b), after 16 experiments, N-ASRSM reduces the size of initial factor space by 44% and, after 22 experiments, it reaches the shrinkage rate of around 100%, which clearly demonstrates the convergence rate of the proposed method. Using the 22 experiments in Table III(b), N-ASRSM fit a quadratic regression with  $R^2_{adj} = 75.32$  and the estimated optimal impactor setting of  $EO = [-1.47, -2.00, 2.00, -2.00]$  (Also see the fitted quadratic surfaces of CCD in A.2). To check the credibility of the comparing methods results, we put all the experiments in Table III(a) and (b)

**Table VI.** Optimality gap trials 7, 8, and 9 of the responses with two variables; trials 11, 12, and 13 of the responses with three variables; and trials 34, 35, and 36 of the responses with six variables

Exp. no.	No obs.	Optimality gap						
		CCD	BBD	N-ASRSM	D-Opt.	V-Opt.	A-Opt.	O-ASRSM
1.1	7	70.52	N/A	0.01	<b>0.00</b>	0.61	40.19	0.07
	8	70.52	N/A	0.72	0.53	0.76	29.94	<b>0.06</b>
	9	70.52	N/A	<b>0.00</b>	7.69	0.83	8.24	0.01
1.2	7	909.82	N/A	0.31	0.31	0.31	1260.68	<b>0.23</b>
	8	909.82	N/A	0.31	0.31	0.31	492.09	<b>0.25</b>
	9	909.82	N/A	<b>0.30</b>	0.31	0.31	5.00	<b>0.30</b>
1.3	7	874.36	N/A	30.79	<b>16.50</b>	<b>16.50</b>	790.25	<b>16.50</b>
	8	756.48	N/A	<b>16.50</b>	<b>16.50</b>	<b>16.50</b>	3583.36	<b>16.50</b>
	9	900.70	N/A	<b>16.50</b>	696.57	<b>16.50</b>	779.73	<b>16.50</b>
2.1	11	25.00	25.46	<b>21.89</b>	23.99	26.16	32.82	23.16
	12	25.05	23.51	<b>22.10</b>	24.06	26.51	33.21	22.13
	13	27.84	22.44	22.03	23.17	26.19	32.92	<b>22.02</b>
2.2	11	19.30	20.28	<b>0.90</b>	6.39	1.40	1.43	2.51
	12	19.30	20.64	1.03	6.37	1.37	1.41	<b>1.02</b>
	13	19.53	19.75	1.08	6.40	1.39	1.43	<b>1.06</b>
3.1	34	3.94	2.06	0.96	0.46	<b>0.17</b>	0.46	0.57
	35	6.65	2.00	<b>0.17</b>	<b>0.17</b>	0.23	<b>0.17</b>	<b>0.17</b>
	36	6.67	4.20	<b>0.13</b>	0.19	0.23	0.19	0.15
3.2	34	4.94	4.24	0.06	0.19	0.09	<b>0.04</b>	0.06
	35	4.63	4.24	<b>0.04</b>	0.07	0.09	<b>0.04</b>	<b>0.04</b>
	36	4.63	4.24	<b>0.02</b>	0.07	0.05	0.03	<b>0.02</b>

CCD: central composite design; BBD: Box-Behnken design; N-ASRSM: *n*-dimensional adaptive sequential response surface methodology; D-Opt.: D-optimal; V-Opt.: V-optimal; A-Opt.: A-optimal; O-ASRSM: optimal adaptive sequential response surface methodology; N/A: not applicable.

**Table VII.** Nonlinear response models used in the simulated experiments

No. of variables	Res. no.	Response relation	Error
Two variable response	1.1	$W = y - \left(\frac{1}{8\pi^2}x^2\right) + \left(\frac{10}{\pi}\right)(x - 2)^2 + 10\left(3 - \frac{1}{12\pi}\right)\cos(x) + \varepsilon$	$N(0,3.5)$
	1.2	$W = 0.75(x - 0.15)^2 + 0.25(x - 0.15)^4 + 1.3(x - 0.15)^6 + 1.8(x - 0.15)(y - 1)^2 - 2.66(y - 1)^2 + 1.9(y - 0.15)^2 + \varepsilon$	$N(0,2)$
Three variable response	2.1	$W = (x - 0.55)^2 + (y + 0.7)^2 + (z - 0.33)^2 - \cos(18(x - 0.55)) - \cos(18(y + 0.7)) - \cos(18(z - 0.33)) + \varepsilon$	$N(0,2)$
	2.2	$W = (x - 1)^3 - 3(y - 1)^3 + (z + 1)^3 - 2(x - 1)^2 - 2(y - 1)^2 + (z + 1)^2 - (x - 1) + 5(y - 1) + 6(z + 1) + 2(x - 1)(y - 1) + (x - 1)(z + 1) - 4(y - 1)(z + 1) + 1 + \varepsilon$	$N(0,1)$
	2.3	$W = x^2 + \exp\left(\frac{y}{10} + 10\right) + \sin(zy) + \varepsilon$	$N(0,3)$
Six variable response	3.1	$W = 6.6(t - 2)^4(u - 1.1)^2 + \frac{3.6(v - 1.35)^6}{((x - 2.3)^2 + 1)} + 1.5(x - 2.3)(y - 1.1)^2(z - 0.25)^4 + \varepsilon$	$N(0,2)$
	3.2	$W = -\exp(-1(10(t - 0.1312)^2 + 3(u + 0.1696)^2 + 17(v - 0.5569)^2 + 3.5(x - 0.0124)^2 + 1.7*(y + 0.8283)^2 + 8(z - 0.5886)^2)) - \exp(-1(0.05(t - 0.2329)^2 + 10(u + 0.4135)^2 + 17(v - 0.8307)^2 + 0.1(x - 0.3736)^2 + 0.8(y + 0.1004)^2 + 14(z - 0.9919)^2)) + \varepsilon$	$N(0,1)$

**Table VIII.** Optimality gap for trials 7, 8, and 9 of the responses with two variables; trials 11, 12, and 13 of the responses with three variables; and trials 34, 35, and 36 of the responses with six variables

		Optimality gap										
f(x)	Run	CCD	BBD	N-ASRSM	RBF	EGO	Standler <i>et al.</i> <sup>29</sup>	Wang <i>et al.</i> <sup>28</sup>	D-optimal	A-optimal	V-Optimal	O-ASRSM
1.1	7	438.43	N/A	0	0	0	0.03	633.55	0.01	0.1	0	0.07
	8	174.6	N/A	0	0	0	668.52	403.37	0	0.1	0	0.01
	9	0.02	N/A	0	0	0	668.24	917.63	0.04	1.18	0.01	0
1.2	7	964.35	N/A	6.48	3.1	4.92	6.27	226.22	171.41	3.1	13.44	4.78
	8	436.18	N/A	4.02	4.01	3.81	589.92	383.74	181.93	5.18	4.55	3.52
	9	5.32	N/A	3.56	3.94	3.81	982.38	197.61	182.05	5.56	6.7	4.75
2.1	11	35.26	81.08	14.93	7.08	7.07	13.64	39.95	10.08	14.75	18.97	14.79
	12	32.03	17.07	6.21	5.78	5.44	97.05	11.51	16.2	13.62	14.6	5.47
	13	89.84	24.54	2.46	1.11	3.51	105.9	12.77	28.89	13.44	18.24	2.86
2.2	11	161.85	299.34	5.08	2.13	2.32	6.2	194.53	1.58	6.91	2.13	5.88
	12	71.22	31.8	2.92	2.18	2.06	92.97	21.67	2.68	7.55	3.57	2.17
	13	120.27	4.06	2.4	2.77	2.15	151.54	0.03	2.83	6.66	35.41	2.04
2.3	11			1.90E+07	3.20E+07	1.90E+07	3.10E+07	1.90E+07				1.90E+07
			7.90E+06	1.90E+07	3.10E+07	2.90E+07	9.86	1.10E+07	0.71	3.10E+07	2.90E+07	2.01E+07
	12	0.67	5.20E+07	3.20E+07	0.74	601.18	9.86	1.10E+07	0.4	3.20E+07	2.90E+07	3.00E+07
13			2.10E+07	0.37	11.77	6.15	1.10E+07	0.4	3.20E+07	2.90E+07	3.10E+07	
3.1	34	295.76	300.76	225.69	230.69	210.52	282.53	242.07	245.62	240.49	213.44	223.96
	35	296.69	290.56	177.82	124.43	117.52	285.79	241.74	241	240.47	107.87	143.67
	36	296.69	290.57	104.1	105.78	104.33	293.37	232.28	245.01	240.47	121.31	106.18
3.2	34	1.67	1.64	0.99	0.97	0.97	1.42	1.01	0.98	1.02	0.98	0.99
	35	1.41	1.65	0.92	0.91	0.9	1.76	1.05	0.98	0.96	0.96	0.91
	36	1.52	1.52	0.88	0.98	0.98	1.82	0.95	0.97	0.98	0.96	0.87

CCD: central composite design; BBD: Box-Behnken design; N-ASRSM: *n*-dimensional adaptive sequential response surface methodology; RBF: radial basis function; EGO: efficient global optimization; O-ASRSM: optimal adaptive sequential response surface methodology.

together and use RBF neural nets to fit a surrogate model as represented in Figure A.3. We also used genetic algorithm (GA) to find the minimum of the surrogate model  $O = [-1.1526, -2.00, 2.00, 2.00]$ , which is considerably closer to the estimate of N-ASRSM.

#### 4.2. Quadratic response models

We now describe the simulated experiments performed to compare the performance of the proposed N-ASRSM approach with those of CCD, BBD, A-optimal, D-optimal, and V-optimal designs, and O-ASRSM method<sup>33</sup> on quadratic response models. We have considered three problems with two variables, three problems three variables, and two problems with six variables. These problems cover different type functions and a range of standard deviation for the error (Table IV). As noted earlier, all response models have a quadratic relation with a normal error term  $\varepsilon \sim N(0, \sigma^2)$ .

Whereas the N-ASRSM and O-ASRSM are adaptive sequential methods, the CCD, BBD, A-optimal, D-optimal, and V-optimal designs are essentially preset designs. To evaluate the effect of this difference, we initially fixed the number of design points at 7 for cases with two variables, 11 for cases with three variables, and 34 for the cases with six variables and then incrementally added two more design points one at a time. For optimal designs, the initial set of design points is optimally generated by optimizing the optimality criteria over the starting factor space with a fine grid system spaced with 0.01 intervals. Next, each of the additional points is generated by optimizing the optimality criterion given the existing design points and the response model. For the CCD and BBD, we initially used 7, 11, or 34 of the full design by excluding some of the points and then re-including them one at a time. For fair comparison, the location of additional points in CCD and BBD are chosen based on their closeness to the direction of maximum improvement.

For the analysis, we have studied the performances in terms of average  $R_{adj}^2$  and average optimality gap (i.e., deviation from the optimal response). All simulated experiments are repeated four times, and average results are reported. The starting factor space is considered with the range of  $[-3, 3]$  in all dimensions for both two and three variable examples. Table V presents the average  $R_{adj}^2$  performances for the consecutive trials.

Table V shows that N-ASRSM is competitive in  $R_{adj}^2$  performance with the rest of the methods. In particular, when the number of experiments is limited, N-ASRSM along with O-ASRSM are consistently the best methods in terms of  $R_{adj}^2$ . Table VI presents the optimality gap results of the consecutive trials of the comparing methods. The optimality gap is measured as the deviation of the response at the final EO from the response at true optimal experiment O. The experiments show that the optimality gap performance of the proposed N-ASRSM is almost the same as O-ASRSM and the most competitive among all methods.

#### 4.3. Nonlinear response models

Here, we compare the performance of the proposed N-ASRSM approach with four global optimization methods including: Standler *et al.*<sup>29</sup>, Wang *et al.*<sup>28</sup>, EGO,<sup>37</sup> a RBF method,<sup>52</sup> and O-ASRSM method,<sup>33</sup> and classical methods CCD, BBD, and A-optimal, D-optimal, and V-optimal designs on five nonlinear response models with two and three variables, with different variance and function type. These response models are presented in Table VII.

For the following analysis, we have examined the performances based on average optimality gap and Euclidian distance of the estimated optima to the real optimal point. All simulated experiments are repeated three times, and average results are reported. To keep the consistency with the preceding section, the result of trials 7, 8, 9 of the cases with two variables, trials 11, 12, and 13 of the cases with three variables, and trials 33, 34, and 35 of cases with six variables have been reported. Table VIII shows the average optimality gap results of the consecutive trials of the comparing methods. The results demonstrate that N-ASRSM is almost as competitive as the best of global optimization approaches, namely EGO and RBF, and better than Standler *et al.*<sup>29</sup>, and Wang *et al.*<sup>28</sup>. Another interesting observation is that, as expected, the rate of improvement (by adding new observations) in the N-ASRSM is more than any other methods in general.

Table IX shows the average Euclidean distance of the estimated optima to the real optima of the underlying function for different methods. Interestingly, the comparison of results in Tables VIII and IX reveals that some of the estimated optima (EOs) that are further away from the real optima (Os) attain better responses than those EOs closer to the Os. Our subsequent analyses indicate that whereas some EOs can be further away from O, they attain better average response due to curvature variation of the response around the O.

## 5. Conclusions

In this paper, we have developed and presented an adaptive methodology for  $n$ -dimensional quadratic response surface optimization. The proposed approach combines concepts from nonlinear optimization, design of experiments, and response surface optimization. The N-ASRSM is a sequential adaptive experimentation approach and uses the information gained from previous experiments to design the subsequent experiment by simultaneously reducing the region of interest and identifying factor combinations for new experiments. Its major advantage is the experimentation efficiency such that, for a given response target, it identifies the input factor combination (or containing region) in a smaller number of experiments than the classical single-shot RSM designs. It differs from earlier studies in its optimality (under certain assumptions), inheritance of results from previous experiments, and robustness due to experiment ranking-based reduction of the region of interest. Through large set simulated experiments, we showed that in modeling quadratic responses it outperforms the popular CCD, BBD, and optimal designs in terms of optimality. Based on another set of simulations, we also showed that N-ASRSM performs well in comparison with global optimization

**Table IX.** The average Euclidean distance to the optimum for the trials 7, 8, and 9 of the responses with two variables; the trials 11, 12, and 13 of the responses with three variables; and the trials 34, 35, and 36 of the responses with six variables

f(x)	Run	Euclidean distance to the optimum										
		CCD	BBD	N-ASRSM	RBF	EGO	Standler <i>et al.</i> <sup>29</sup>	Wang <i>et al.</i> <sup>28</sup>	D-optimal	A-optimal	V-Optimal	O-ASRSM
1.1	7	2.43	N/A	<b>0.01</b>	<b>0.01</b>	<b>0.01</b>	0.05	1.84	0.09	0.31	<b>0.01</b>	0.26
	8	1.65	N/A	0.01	0.01	<b>0</b>	3.17	2.56	<b>0</b>	0.32	<b>0</b>	<b>0</b>
	9	0.13	N/A	<b>0</b>	0.01	<b>0</b>	3.17	3.01	0.19	1.09	0.01	0.05
1.2	7	3.01	N/A	0.67	0.79	0.65	0.51	0.96	1.11	<b>0.39</b>	0.58	0.45
	8	1.97	N/A	<b>0.41</b>	41	0.43	2.02	2.2	1.17	0.46	0.44	<b>0.42</b>
	9	0.45	N/A	<b>0.38</b>	0.46	0.42	2.39	1.73	1.17	0.47	0.5	<b>0.43</b>
2.1	11	1.09	2.18	0.91	0.38	0.32	0.42	1.2	0.31	0.83	1.09	<b>0.3</b>
	12	1.06	1.3	0.72	0.36	<b>0.3</b>	2.01	0.38	1.02	0.89	1.37	0.69
	13	1.53	0.62	<b>0.3</b>	0.35	<b>0.3</b>	2.25	0.32	1.21	0.97	1.11	0.43
2.2	11	2.02	2.69	0.59	<b>0.34</b>	<b>0.34</b>	0.9	1.95	0.54	0.55	0.79	0.7
	12	1.34	0.99	0.55	0.26	<b>0.22</b>	3.33	0.69	0.6	0.66	0.81	0.57
	13	1.07	0.46	0.35	0.34	0.35	3.87	<b>0.19</b>	0.58	0.86	0.77	0.53
2.3	11	0.48	1.76	0.79	0.39	0.41	<b>0.32</b>	3.21	0.63	0.47	0.67	0.48
	12	2.23	1.59	0.29	0.14	<b>0.13</b>	2.95	0.39	0.7	0.41	0.74	0.2
	13	2.06	0.88	<b>0.13</b>	0.14	<b>0.13</b>	3.12	0.7	0.7	0.39	0.34	0.15
3.1	34	8.56	8.06	5.11	5.85	<b>4.77</b>	8.45	5.12	5.29	5.86	5.13	5.91
	35	8.31	8.78	<b>4.08</b>	4.91	4.73	8.01	5.09	5.17	5.87	4.88	<b>4.08</b>
	36	8.3	8.75	4.01	<b>3.98</b>	4.02	8.7	4.96	5.2	5.87	4.99	4.03
3.2	34	6.4	6.64	3.18	3.75	<b>2.47</b>	6.34	5.1	5.02	6	5.73	5.43
	35	6.64	6.63	3.99	<b>2.43</b>	2.47	6.84	5.21	4.92	5.98	5.73	4.06
	36	6.37	6.64	2.51	2.07	<b>1.47</b>	6.98	4.93	4.96	5.96	5.73	3.54

CCD: central composite design; BBD: Box–Behnken design; N-ASRSM: *n*-dimensional adaptive sequential response surface methodology; RBF: radial basis function; EGO: efficient global optimization; O-ASRSM: optimal adaptive sequential response surface methodology; N/A: not applicable.

approaches in estimating the optima of nonlinear responses. For future studies, the proposed methodology could be extended to higher order of response functions.

## References

1. Box GEP, Wilson KB. On the experimental attainment of optimum conditions. *Journal of the Royal Statistical Society* 1951; **13**:1–15.
2. Box GEP, Hunter WG, Hunter JS. *Statistics for Experimenters: Design, Innovation, and Discovery*, 2nd Edition, NY: John Wiley and Sons, 2005.
3. Sanchez SM, Sanchez PJ. Very large fractional factorial and central composite designs. *ACM Transactions on Modeling and Computer Simulation (TOMACS)* 2005; **15**(4):362–377.
4. Box GEP, Behnken DW. Some new three level design for the study of quantitative variables. *Technometrics* 1960; **2**:455–476.
5. Box GEP. Statistics as a catalyst to learning by scientific method: Part II – a discussion. *Journal of Quality Technology* 1999; **31**(1):16–29.
6. Myers RH, Khuri AI, Carter WH. Response surface methodology: 1966–1988. *Technometrics* 1989; **31**:137–157.
7. Myers RH. Response surface methodology—current status and future directions. *Journal of Quality Technology*, 1999; **31**:30–44.
8. Myers RH, Montgomery DC, Vining CG, Borror CM, Kowalski SM, Response surface methodology: a retrospective and literature survey, *Journal of Quality Technology* 2004; **36**:53–77.
9. Montgomery DC. *Design and Analysis of Experiments*, 7th Ed, NJ: John Wiley & Sons, 2008.
10. Draper RD. Small composite designs. *Technometrics* 1985; **27**(2):173–180.
11. Myers RH, Montgomery DC. *Response Surface Methodology*, NY: John Wiley & Sons, 1995.
12. Kiefer J. Optimum experimental designs. *Journal of Royal Statistical Society B* 1959; **21**:272–304.
13. Kiefer J. Optimum designs in regression problems. *Annals of Mathematical Statistics* 1961; **32**:298–325.
14. Kiefer J, Wolfowitz J. Optimum designs in regression problems. *Annals of Mathematical Statistics* 1959; **30**:271–294.
15. Andere-Rendon J, Montgomery DC, Rollier DA. Design of mixture experiments using Bayesian D-optimality. *Journal of Quality Technology* 1997; **29**(4):451–463.
16. Joshi SH, Sherali HD, Tew JD. An enhanced response surface methodology (RSM) algorithm using gradient deflection and second order search strategies. *Computers and Operations Research*, 1998; **25**(7/8):531–541.
17. Kleijnen JPC, Hertog DD, Angun ME. Response surface methodology's steepest ascent and step size revisited. *European Journal of Operational Research* 2004; **159**(1):121–131.
18. Kleijnen JPC, Hertog DD, Angun ME. Response surface methodology's steepest ascent and step size revisited: correction. *European Journal of Operational Research* 2006; **170**(2):664–666.
19. Box GEP. Evolutionary operation: a method for increasing industrial productivity. *Applied Statistics* 1957; **6**:81–101.
20. Box GEP, Draper NR. *Evolutionary Operation: A Method for Increasing Industrial Productivity*. NY: John Wiley and Sons, 1969.
21. Spendley GR, Hex GR, Himsforth FR. Sequential application of simplex designs in optimization and evolutionary operation. *Technometrics* 1962; **4**:441–461.
22. Friedman M, Savage LJ. *Planning Experiments Seeking Maxima*. In *Techniques of Statistical Analysis*, edited by Eisenhart C, Hastay M, Wallis WA, NY: McGraw-Hill; 1947, 363–72.
23. Czitrom V. One-factor-at-a-time versus designed experiments. *The American Statistician* 1999; **53**(2):126–131.
24. Frey DD, Engelhardt F, Greitzer EM. A role for 'one-factor-at-a-time' experimentation in parameter design. *Research in Engineering Design* 2003; **14**:65–74.
25. Frey DD, Jugulum, R. The mechanisms by which adaptive one-factor-at-a-time experimentation leads to improvement. *American Society of Mechanical Engineers Journal of Mechanical Design* 2006; **128**:1050–1060.
26. Frey DD, Wang H. Adaptive one-factor-at-a-time experimentation and expected value of improvement. *Technometrics* 2006; **48**(3):418–31.
27. Wang G, Dong Z, Aitchison P. Adaptive response surface method—a global optimization scheme for computation-intensive design problems. *Journal of Engineering Optimization* 2001; **33**(6):707–734.
28. Wang G. Adaptive response surface method using inherited Latin hypercube designs. *American Society of Mechanical Engineers Journal of Mechanical Design* 2003; **125**(2):210–220.
29. Sandler N. The successive response surface method applied to sheet-metal forming, Proceedings of the First MIT Conference on Computational Fluid and Solid Mechanics, Boston, June 12–14, 2001. Elsevier Science Ltd., Oxford.
30. Moore AW, Schneider JM, Boyan J, Lee MS. Q2: a memory based active learning algorithm for black box noisy optimization. Proceedings of the Fifteenth International Conference on Machine Learning, 1998; 386–394 Morgan Kaufmann.
31. Anderson, BS, Moore AW, Cohn D. A nonparametric approach to noisy and costly optimization. *Proceedings of the Seventeenth International Conference on Machine Learning (ICML)* 2000, Santa Clara, CA, USA.
32. Alaeddini A, Murat, A, Yang K, Ankenman B. An efficient adaptive sequential methodology for expensive response surface optimization. *Quality and Reliability Engineering International* 2013; to appear.
33. Alaeddini A, Yang K, Murat A. ASRSM: A sequential experimental design for response surface optimization. *Quality and Reliability Engineering International* 2013; **29**(2):241–258.
34. Sobieszcanski-Sobieski, J. Optimization by decomposition: a step from hierarchic to nonhierarchic systems, Second NASA/Air Force Symposium on Recent Advances in Multidisciplinary Analysis and Optimization, Hampton, VA, NASA CP-3031, Part 1. Also NASA TM-101494, 1988.
35. Renaud JE, Gabriele GA. Approximation in non-hierarchic system optimization. *American Institute of Aeronautics and Astronautics Journal* 1994; **32**(1):198–205.
36. Rodriguez JF, Renaud, JE, Watson LT. Convergence of trust region augmented Lagrangian methods using variable fidelity approximation data. *Structural and Multidisciplinary Optimization* 1998; **15**:141–156.
37. Jones DR, Schonlau M, Welch WJ. Efficient global optimization of expensive black-box functions. *Journal of Global Optimization* 1998; **13**(4):455–492.
38. Alexandrov NM, Dennis JE, Lewis RMV. A trust region framework for managing the use of approximation models in optimization. *Structural and Multidisciplinary Optimization* 1998; **15**(1):16–23.
39. Chang KH, Hong J, Wan H. Stochastic trust-region response-surface method (STRONG)—a new response-surface framework for simulation optimization, *INFORMS Journal on Computing*, 2012; To appear.
40. Gano SE, Renaud JE. Variable fidelity optimization using a kriging based scaling function, 10th AIAA/ISSMO Multidisciplinary Analysis and Optimization Conference, 30 August – 1 September 2004, Albany, New York, 2004.
41. Rodriguez JF, Perez VM, Padmanabhan D, Renaud, JE. Sequential approximate optimization using variable fidelity response surface approximations. *Structural Optimization* 2001; **22**(1):24–34.
42. Jones DR. A taxonomy of global optimization methods based on response surfaces. *Journal of Global Optimization*, 2001; **21**(4):345–383.

43. Sobieszcanski-Sobieski J, Haftka RT. Multidisciplinary aerospace design optimization: survey of recent developments. *Structural and Multidisciplinary Optimization* 1997; **14**(1):1–23.
44. Kleijnen JPC. Simulation experiments in practice: statistical design and regression analysis. *Journal of Simulation* 2008; **2**(1):19–27.
45. Kleijnen JPC, Beers WCMV, Nieuwenhuysse IV. Constrained optimization in simulation: a novel approach. *European Journal of Operational Research* 2010; **202**(1):164–174.
46. Simpson TW, Booker AJ, Ghosh D, Giunta AA, Koch PN, Yang RJ. Approximation methods in multidisciplinary analysis and optimization: a panel discussion. *Structural and Multidisciplinary Optimization* 2004; **27**(5):302–313.
47. Chen VCP, Tsui KL, Barton RR, Meckesheimer M. A review on design, modeling and applications of computer experiments, *IIE Transactions* 2006; **38**:273–291.
48. Walters FS, Parker Jr, LR, Morgan, SL, Deming SN. *Sequential Simplex Optimization for Quality & Productivity in Research, Development, and Manufacturing*. FL: CRC Press, 1991.
49. Tan PN, Steinbach M, Kumar V. *Introduction to Data Mining*. NY: Addison-Wesley, 2006.
50. Richards FJ. A flexible growth function for empirical use. *Journal of Experimental Botany* 1959; **10**:290–300.
51. Seber GAF, Alan JL. *Linear Regression Analysis*. NJ: Wiley Interscience, 2003.
52. Gutmann HM. A radial basis function method for global optimization. *Journal of Global Optimization* 2001; **19**(3):201–227.
53. Faul M, Xu L, Wald MM, Coronado VG. *Traumatic Brain Injury in the United States: Emergency Department Visits, Hospitalizations, and Deaths*. In. Atlanta (GA): Centers for Disease Control and Prevention, National Center for Injury Prevention and Control, 2010.
54. Mauritz W, Wilbacher I, Majdan M, Leitgeb J, Janciak, I, Brazinova A, Rusnak M. Epidemiology, treatment and outcome of patients after severe traumatic brain injury in European regions with different economic status. *European Journal Public Health* 2008; **18**(6):575–580.
55. Mao H, Zhang L, Yang KH, King AI. Application of a finite element model of the brain to study traumatic brain injury mechanisms in the rat. *Stapp Car Crash Journal* 2006; **50**:583–600.
56. Mao H, Yang KH, King AI, Yang K. Computational neurotrauma—design, simulation, and analysis of controlled cortical impact model. *Biomechanics and Modeling in Mechanobiology* 2010; **9**(6):763–772.
57. Varian H. Bootstrap tutorial. *Mathematica Journal* 2005; **9**:768–775.
58. Bazaraa MS, Goode JJ. An algorithm for solving linearly constrained mini-max problems, *European Journal of Operational Research* 1982; **11**:158–166.
59. Dutta RSK, Vidyasagar M. New algorithm for constrained mini-max optimization. *Mathematical Programming* 1977; **13**:140–155.
60. Lemarechal C. Nondifferentiable optimization. *Handbooks in Operations Research and Management Science*, Edited by Nemhauser GL, Rinnooy Kan AHG, Todd MJ, Elsevier Science Publishers: Amsterdam, Holland; 1989, **1**:529–572
61. Madsen K, Schjaer-Jacobsen H. Linearly constrained mini-max optimization, *Mathematical Programming* 1978; **14**:208–223.
62. Vincent TL, Goh BS, Teo KL. Trajectory-following algorithms for mini-max optimization problems. *Journal of Optimization Theory and Applications* 1992; **75**:501–519.

**Appendix A. Traumatic brain injury: injury level graphs estimated using radial basis function, central composite design, and  $n$ -dimensional adaptive sequential response surface methodology**

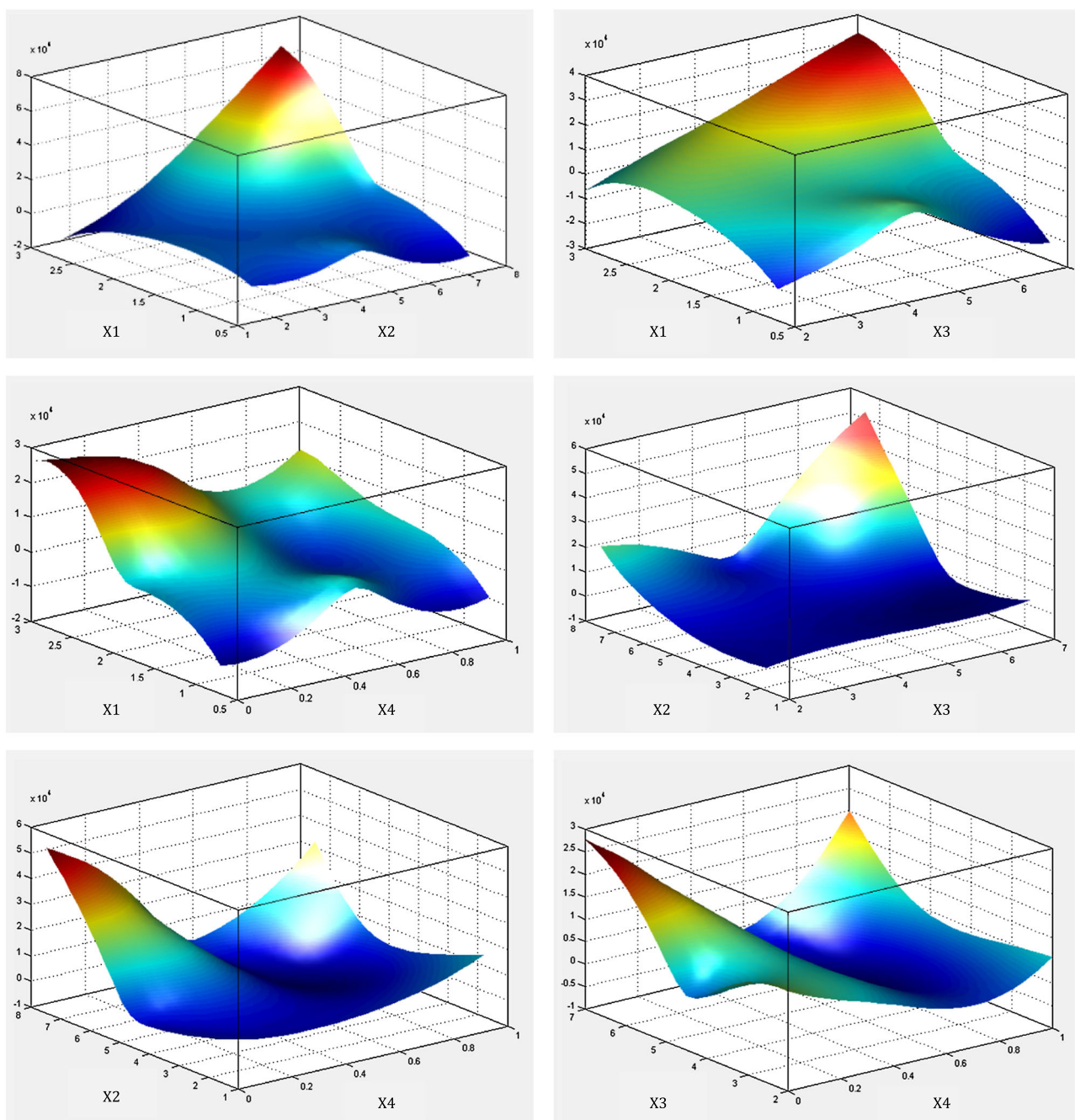


Figure A.1. The fitted surface using radial basis function based on all data together

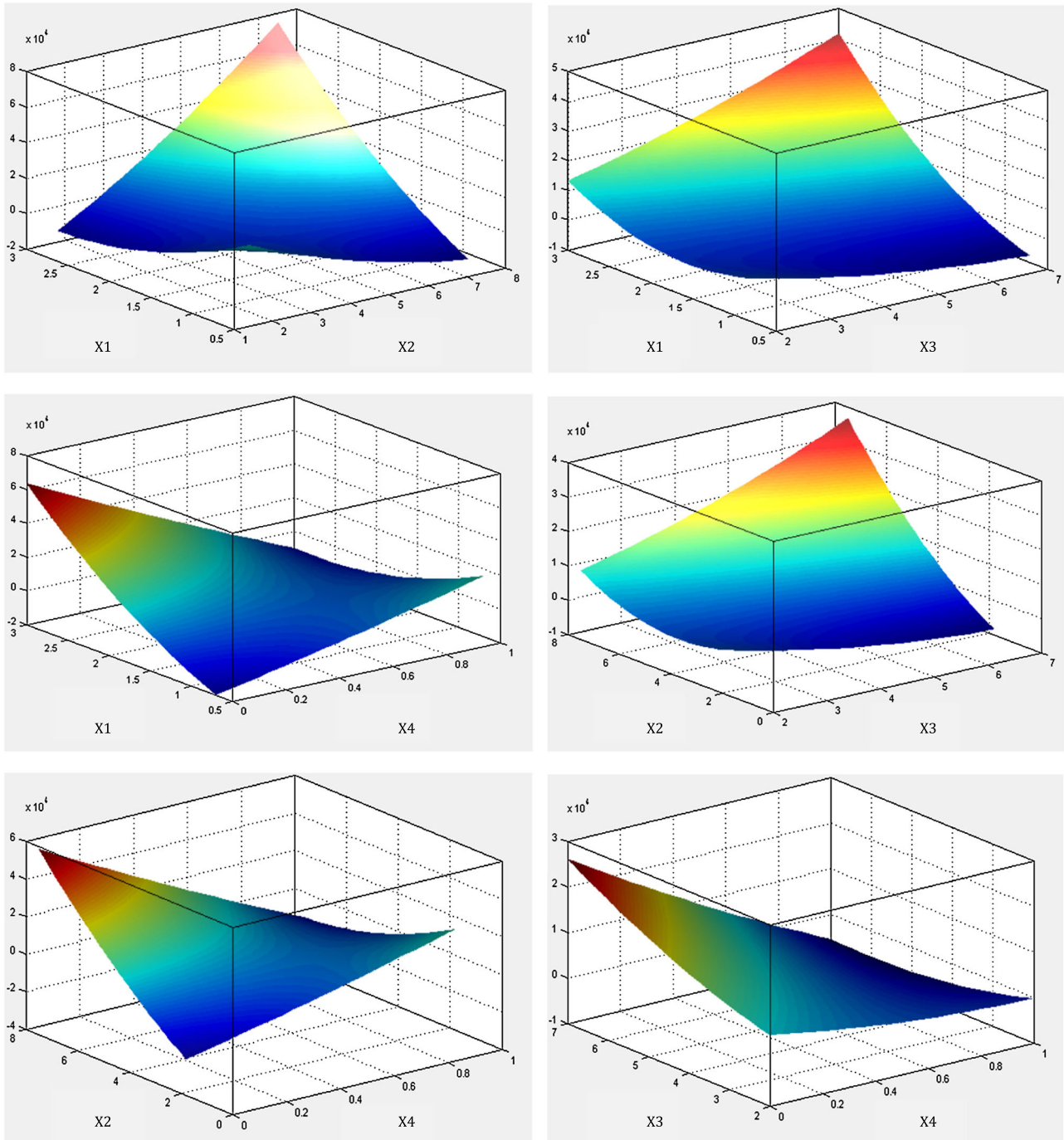


Figure A.2. The fitted surface based on central composite design

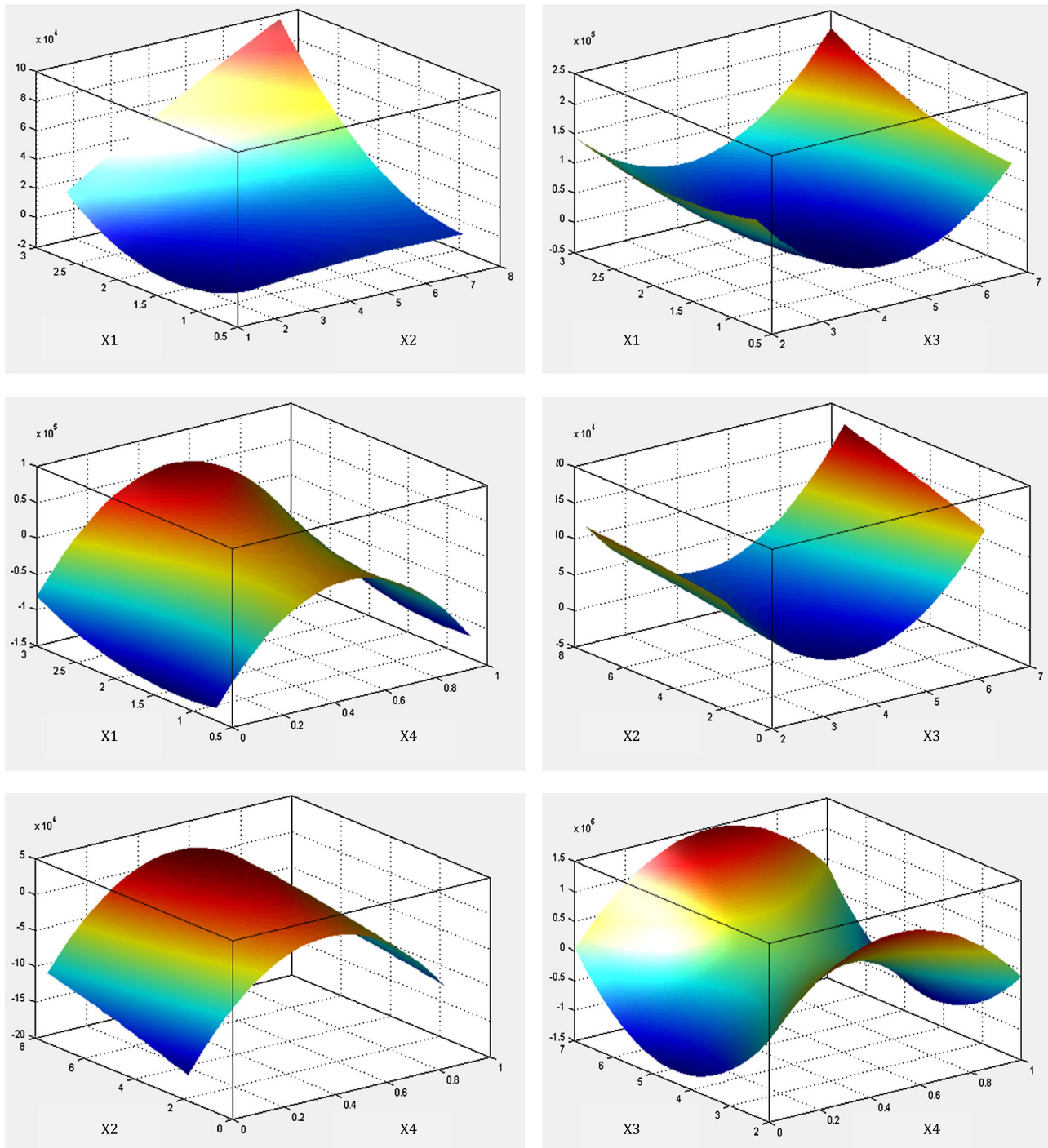


Figure A.3. The fitted surface based on n-dimensional adaptive sequential response surface methodology design

## Appendix B. Convergence analysis of nonparametric approach

Here, we study the convergence the nonparametric approach for various dimensions (given that the result of ranking of experiments is correct). Because the proposed approach provides the exact amount of shrinkage in the factor space (*FS*), to find the overall performance of nonparametric strategy, we can simply consider all possible (ranking) scenarios and have the average. However, as the dimension increases, the numbers of possible scenarios rise drastically, which makes it very difficult to check all scenarios in higher dimensions (Table B1).

**Table B1.** Number of possible scenarios versus number of dimensions; possible permutations of experiment's rankings

No. of dimensions	Number of possible corner points	Number of starting points in the initial design $D$	Possible ranking of experiments	Number of possible point to be experimented (to complete the design)	Possible permutations of ranking after adding the $y^{\text{th}}$ experiment	Possible rankings after adding $P$ experiments
$n$	$T = 2^n + 2n + 1$	$e = \begin{cases} 2^n + 1 & n = 2 \\ 2^{n-1} + 1 & n > 2 \end{cases}$	$e!$	$P = T - e$	$e! \times [P \times \dots \times (P - y + 1)] \times [(e + 1) \times \dots \times (e + y)]$	$e! \times T!$
2	9	5	120	4	$y = 2$ 60480	43545600
3	15	7	5040	8	322560 20321280	6.591E + 15
4	25	15	1.308E + 12	10	2.09228E + 14 3.20119E + 16	2.028E + 37

To address this problem we use bootstrapping (Varian<sup>57</sup>) from the vast number of possible ranking permutations to find the empirical estimate of the shrinkage rate of the nonparametric strategy.

To implement bootstrapping, we take the following steps: (i) take a large random sample (with replacement) from the pool of all possible ranking scenarios (for each choice of dimensionality, e.g.,  $n = 2, 3, \dots$ ) and use that sample as the base dataset of bootstrap sampling; (ii) construct a number of bootstrap samples of the same size of the base dataset, by random sampling with replacement from the base dataset; (iii) find the average rate of shrinkage in each bootstrap sample; and (iv) use the mean of shrinkage rates from different bootstrap samples as the estimated rate of shrinkage of the proposed nonparametric approach for different dimensions. Table B2 illustrates the result of bootstrapping over different dimensions.

Table B2. The result of bootstrap sampling for different number of dimensions		
No. of dimensions	Experiment	Percentage of reduction (%)
2	5	62
	6	62
	7	80
	8	91
	9	91
3	5	1
	6	8
	7	16
	8	26
	9	52
	10	67
	11	84
	12	93
4	13	94
	14	98
	9	40
	10	45
	11	47
	12	41
	13	45
	14	30
	15	44
	16	64
	17	81
	18	89
	19	94
	20	99

In Table XI, when the ranking of the experiments is correct which can usually happen when error size is not very significant, the convergence rate of the proposed approach is considerable. Indeed the proposed nonparametric strategy is often able to find an acceptably small optimal subregion within the initial factor space ( $FS_1$ ), before completing the full factorial design. It should be mentioned that the very appealing convergence rate of the proposed approach is at the expense of higher computation complexity comparing to typical RSM methodologies which is discussed in detail in Appendix C.

### Appendix C. Computational complexity of the proposed methodology

The computational complexity of the proposed methodology has many folds; however, the most contributing components include: (i) nonparametric approach; (ii) parametric approach; and (iii) risk adjustment. Figure B.1 illustrates the structure of the main components of the N-ASRSM.

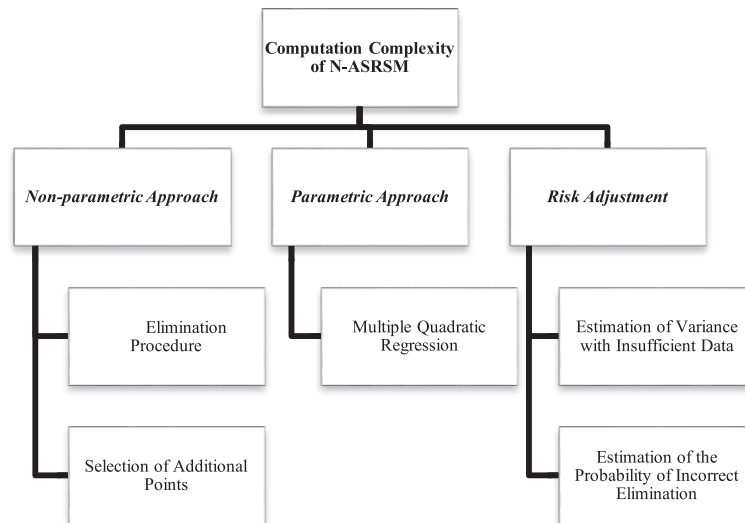


Figure C.1. The structure of the components adding to the complexity of the n-dimensional adaptive sequential response surface methodology

#### Nonparametric approach complexity

In Figure B.1, nonparametric approach has two major parts: (i) *NOR* elimination procedure and (ii) selection of additional point. The core step in *NOR* elimination procedure is solving a cubic polynomial min–max (continuous) optimization problem for each subregion to decide if it contains *RO* or not. This problem can be solved by efficient polynomial order algorithms.<sup>58–62</sup> However, the number of subregions investigated by min–max optimization is  $2^n$ , where  $n$  is the number of dimensions (factors). As a result, the overall complexity of the *NOR* elimination procedure is exponential in time.

When *NOR* elimination procedure terminates without a candidate hyper-rectangular *FS* or very small eliminated subregion, then additional points are selected based *additional point selection procedure* to enable eliminating more of the *NOR* subregions. *Additional point selection procedure* first uses cosine similarity measure to calculate the similarity of un-experimented corners to the worst point (*W*), which is linear time algorithm and next identify the most dissimilar un-experimented corner to *W*, which is again a linear time algorithm.

#### Parametric approach complexity

The main part of parametric approach is quadratic regression fitting. For a least squares regression with  $E$  training examples and  $n$  variables (factors), using least square technique, the vector of regression coefficients  $B$  can be gained as  $B = (X^T X)^{-1} X^T Y$ , where  $X$  is the data matrix of experiments' settings and  $Y$  is the vector of associated measurements of the experiments. Calculation of  $B$  includes matrix multiplication and *LU* (or Cholesky) factorization operations, both of them are polynomial time algorithms.

#### Risk adjustment complexity

Risk adjustment has two major parts: (i) estimation of variance (when there is not enough experiments) and (ii) calculating the probability of incorrect ranking. *Estimation of variance* is carried out by solving a system of two linear equations in two variables that requires *SST* calculation as prior, resulting in a linear time complexity. *Estimation of the probability of incorrect ranking* is performed using *Procedure 2*, which is again a linear time algorithm.

As a result, the complexity of the N-ASRSM methodology is exponential due to the nonparametric approach complexity. Indeed, O-ASRSM trades off between the total number of experiments and the computational complexity of the algorithm. Considering the fact that in most practical cases, the required computational effort is negligible, either due to the existence of powerful computational resources (e.g., parallel computing facilities) or due to experiments being too costly vis-à-vis the computational effort; N-ASRSM can be effectively applied in practice.

#### Authors' biographies

**Dr. Adel Alaeddini** is an assistant professor of Mechanical Engineering at University of Texas at San Antonio. He received his Ph.D. in Industrial and Systems Engineering from Wayne State University. His research interests include data mining and statistical learning, quality and reliability engineering, and global optimization, with applications in Healthcare Operations Management, Biomedical

Informatics, and Manufacturing Operations. Dr. Alaeddini has authored over 20 publications in peer reviewed journals and refereed proceedings, and two book chapters. His research has been supported by National Science Foundation (NSF), Department of Veteran Affairs (VA), Chrysler Corporation, and Harland Clarke Corporation.

**Dr. Kai Yang** is a professor in the Department of Industrial and Manufacturing Engineering, Wayne State University. His research areas include statistical methods in quality and reliability engineering, engineering design methodologies, and healthcare system engineering. Dr. Yang has written five books in the areas of Design for Six Sigma, multivariate statistical methods, and voice of the customer and published 70 research papers. Dr. Yang has been awarded over 50 research contracts from such institutions as US National Science Foundation, US Department of Veteran Affairs, Siemens Corp, General Motors Corporation, Ford Motor Company, and Chrysler Corporation. Dr. Yang received an MS degree in 1985 and a PhD degree in industry engineering in 1990, both of them from the University of Michigan.

**Dr. Haojie Mao** is a senior research fellow in the Bioengineering Center of Wayne State University. He received his Ph.D. in Biomedical Engineering from the Wayne State University in 2009. He has broad research and teaching interests in biomechanics, including neurotrauma, human body modeling, biomedical design, pediatric biomechanics, and vehicle safety engineering. He has authored over 20 publications in archival journals and refereed proceedings. His research has been supported by National Highway Transportation Safety Administration (NHTSA), Department of Defense (DOD), Toyota Collaborative Safety Research Center (CSRC), Alternatives Research & Development Foundation (ARDF), China National Science Foundation, and Cervigard, among the others. He has served as assistant session chair for SAE World Congress, Session Organizer for ASME IMECE, guest editor for Internal Journal of Vehicle Safety, editorial board member for the journal *Advances in Biomechanics and Applications*, and ad hoc reviewers for over one dozen of journals and conferences.

**Dr. Alper Murat** is an associate professor of Industrial and Systems Engineering at Wayne State University. He received his Ph.D. in Operations Research and Management Science from the McGill University, Montreal, Canada in 2006. He has research and teaching interests in operations research and predictive analytics, with applications to healthcare and manufacturing operations and supply chain management. He has authored over 30 publications in archival journals and refereed proceedings. His research has also been supported by the National Science Foundation (NSF), US Department of Transportation (US DoT), Department of Veterans Affairs (VA), Department of Homeland Security (DHS), General Dynamics, and Ford Motor Company, among others. He is a member of INFORMS and the Institute of Industrial Engineers (IIE). His students and research received best paper and dissertation awards from IIE, INFORMS, Intelligent Transportation Society in Michigan. He is the chair of SAE's Global Supply Chains and Manufacturing Cluster and has served on the organizing committees of SAE World Congress, IEEE Conference on Technologies for Homeland Security, Land and Maritime Border Security, Complex Adaptive Systems conferences, among others.

**Dr. Bruce Ankenman** is a Charles Deering McCormick Professor of Teaching Excellence at Northwestern University. He is an associate professor in the Department of Industrial Engineering and Management Sciences at Northwestern's McCormick School of Engineering and Applied Sciences. He received a BS in Electrical Engineering from Case Western Reserve University and after working in the automotive industry for 5 years, returned to graduate school for an MS and PhD in Industrial Engineering from the University of Wisconsin-Madison. His research interests primarily deal with the design and analysis of experiments that are used to build models for physical systems or metamodels for simulated systems. Professor Ankenman is the codirector of the Segal Design Institute and for the last 7 years, he has also directed McCormick's well-known freshman design course, Design Thinking and Communication, formerly Engineering Design and Communication.